

## Accelerated Article Preview

# Human leukocyte antigen alleles associate with COVID-19 vaccine immunogenicity and risk of breakthrough infection

Received: 24 December 2021

Accepted: 7 October 2022

Accelerated Article Preview

Published online: 13 October 2022

Cite this article as: Mentzer, A. J. et al. Human leukocyte antigen alleles associate with COVID-19 vaccine immunogenicity and risk of breakthrough infection. *Nature Medicine* <https://doi.org/10.1038/s41591-022-02078-6> (2022).

Alexander J. Mentzer, Daniel O'Connor, Sagida Bibi, Irina Chelysheva, Elizabeth A. Clutterbuck, Tesfaye Demissie, Tanya Dinesh, Nick J. Edwards, Sally Felle, Shuo Feng, Amy L. Flaxman, Eleanor Karp-Tatham, Grace Li, Xinxue Liu, Natalie Marchevsky, Leila Godfrey, Rebecca Makinson, Maireid B. Bull, Jamie Fowler, Bana Alamad, Tomas Malinauskas, Amanda Y. Chong, Katherine Sanders, Robert H. Shaw, Merryn Voysey, Matthew D. Snape, Andrew J. Pollard, Teresa Lambe & Julian C. Knight

This is a PDF file of a peer-reviewed paper that has been accepted for publication. Although unedited, the content has been subjected to preliminary formatting. Nature Medicine is providing this early version of the typeset paper as a service to our authors and readers. The text and figures will undergo copyediting and a proof review before the paper is published in its final form. Please note that during the production process errors may be discovered which could affect the content, and all legal disclaimers apply.

# Human leukocyte antigen alleles associate with COVID-19 vaccine immunogenicity and risk of breakthrough infection

Alexander J Mentzer<sup>1\*</sup>, Daniel O'Connor<sup>2,3\*</sup>, Sagida Bibi<sup>2,3</sup>, Irina Chelysheva<sup>2,3</sup>, Elizabeth A Clutterbuck<sup>2,3</sup>, Tesfaye Demissie<sup>2,3</sup>, Tanya Dinesh<sup>2,3</sup>, Nick J Edwards<sup>4</sup>, Sally Felle<sup>2,3</sup>, Shuo Feng<sup>2,3</sup>, Amy L Flaxman<sup>2,3</sup>, Eleanor Karp-Tatham<sup>1</sup>, Grace Li<sup>2,3</sup>, Xinxue Liu<sup>2,3</sup>, Natalie Marchevsky<sup>2,3</sup>, Leila Godfrey<sup>2,3</sup>, Rebecca Makinson<sup>4</sup>, Maireid B Bull<sup>2,5</sup>, Jamie Fowler<sup>4</sup>, Bana Alamad<sup>1</sup>, Tomas Malinauskas<sup>6</sup>, Amanda Y Chong<sup>1</sup>, Katherine Sanders<sup>2,3</sup>, Robert H Shaw<sup>2,3</sup>, Merryn Voysey<sup>2,3</sup>, Oxford COVID Vaccine Trial Genetics Study Team Group<sup>†</sup>, Matthew D Snape<sup>2,3</sup>, Andrew J Pollard<sup>2,3\*</sup>, Teresa Lambe<sup>2,3,5\*</sup>, Julian C Knight<sup>1,3,5\*</sup>

\*Contributed equally

<sup>†</sup>Members are listed in Appendix 1

<sup>1</sup>Wellcome Centre for Human Genetics, Nuffield Department of Medicine, University of Oxford, Oxford, UK; <sup>2</sup>Oxford Vaccine Group, Department of Paediatrics, University of Oxford, Oxford, UK; <sup>3</sup>NIHR Oxford Biomedical Research Centre and Oxford University Hospitals NHS Foundation Trust, Oxford, UK; <sup>4</sup>The Jenner Institute, Nuffield Department of Medicine, University of Oxford, Oxford, UK; <sup>5</sup>Chinese Academy of Medical Science (CAMS) Oxford Institute, University of Oxford, Oxford, UK; <sup>6</sup>Division of Structural Biology, Wellcome Centre for Human Genetics, University of Oxford, Oxford, UK.

## 32 Abstract

33 SARS-CoV-2 vaccine immunogenicity varies between individuals, and immune responses  
34 correlate with vaccine efficacy. Using data from 1,076 participants enrolled in ChAdOx1  
35 nCov-19 vaccine efficacy trials in the United Kingdom, we find that inter-individual variation  
36 in normalised antibody responses against SARS-CoV-2 spike (S) and its receptor binding  
37 domain (RBD) at 28 days following first vaccination shows genome-wide significant  
38 association with major histocompatibility complex (MHC) class II alleles. The most  
39 statistically significant association with higher levels of anti-RBD antibody was HLA-DQB1\*06  
40 ( $P=3.2 \times 10^{-9}$ ), which we replicate in 1,677 additional vaccinees. Individuals carrying HLA-  
41 DQB1\*06 alleles were less likely to experience PCR-confirmed breakthrough infection during  
42 the ancestral SARS-CoV-2 virus and subsequent Alpha-variant waves compared with non-  
43 carriers (HR 0.63, 0.42-0.93,  $P=0.02$ ). We identify a distinct S-derived peptide that is  
44 predicted to bind differentially to HLA-DQB1\*06 compared with other similar alleles, and  
45 find evidence of increased spike-specific memory B-cell responses in HLA-DQB1\*06 carriers  
46 at 84 days following first vaccination. Our results demonstrate association of HLA type with  
47 COVID-19 vaccine antibody response and risk of breakthrough infection, with implications  
48 for future vaccine design and implementation.

49

## 50 Introduction

51 Since its emergence in late 2019, SARS-CoV-2 has caused a global pandemic with estimates of  
52 between 6.5-15 million deaths up to September 2022<sup>1,2</sup>. Vaccines targeting, predominantly, the  
53 spike (S) antigen of SARS-CoV-2 have demonstrated high efficacy against severe disease in phase 3  
54 trials, eliciting high levels of binding and neutralising antibodies, as well as T cell responses, with  
55 over 12 billion doses administered worldwide<sup>1</sup>. Two of the earliest developed vaccines, BNT162b2

(Pfizer-BioNTech)<sup>3</sup> and ChAdOx1 nCoV-19 (AZD1222; Oxford-AstraZeneca)<sup>4</sup> are estimated to have population effectiveness against a positive PCR test for the earliest variants of SARS-CoV-2 of 79% and 80% respectively when assessed at least 21 days following the second dose of vaccination in a community-based household survey from the United Kingdom (1 December 2020 to 8 May 2021)<sup>5</sup>, together with 88-91% effectiveness against hospital admission for coronavirus disease (COVID-19)<sup>5</sup>, although lower effectiveness is reported with more recent variants of concern<sup>6</sup>. Despite the success of vaccines at reducing mortality and morbidity in the population with effectiveness against severe disease and hospitalisation currently remaining high, vaccine breakthrough infections, while predominantly mild, are increasingly reported<sup>7-9</sup>.

Significant variation in immune responses, including antibody levels and T cell responses, has been reported among vaccinated individuals<sup>10</sup>. Neutralising antibody levels show association with vaccine efficacy in animal challenge studies<sup>11</sup> and humans<sup>12,13</sup>, and risk of symptomatic COVID-19 has been shown to reduce with increasing levels of both anti-spike (anti-S IgG) and antibodies against receptor binding domain (RBD) antigenic sites on the viral spike (anti-RBD IgG) following vaccination with ChAdOx1 nCoV-19<sup>13</sup>. The reasons for inter-individual variation in total or neutralising antibody responses are incompletely understood<sup>10,14</sup>. Community-based surveys have provided some epidemiological insight into this question among individuals with no prior history of SARS-CoV-2 infection in the UK general population: a low anti-spike IgG antibody responder group following vaccination was identified and found to be more commonly male, elderly (over 75 years of age) and with long term health conditions<sup>10</sup>.

We sought to investigate the contribution of genetic factors to the observed variation in response to vaccination with ChAdOx1 nCoV-19. Antibody responses following vaccination show evidence of heritability<sup>15</sup> with genetic variation in HLA within the Major Histocompatibility Complex (MHC) on chromosome 6 (position p21.3) associated with responses to hepatitis B<sup>16-19</sup>, tetanus<sup>20</sup>, and measles<sup>21,22</sup> vaccines. For these infections, the relevance for vaccine failure has not been robustly



demonstrated<sup>23,24</sup>. To date, genetic studies in COVID-19 have focused on risk of severe disease with replicated associations implicating antiviral defence mechanisms (notably involving interferon signalling), mediators of inflammatory organ damage, leucocyte differentiation and blood type antigen secretor status, but limited evidence to date for HLA<sup>25-27</sup>. Here we use data from five clinical trials of ChAdOx1 nCoV-19 to demonstrate association of HLA-DQB1\*06 with higher antibody responses against the RBD of S antigen and lower risk of breakthrough infections, which we propose involves altered HLA-peptide binding influencing memory B-cell responses.

## Results

### Genome-wide association study of antibody responses 28 days after ChAdOx1 nCoV-19 vaccination

We hypothesised that genetic factors contribute to inter-individual variation in COVID-19 vaccine responses. To investigate this, we first performed a discovery analysis testing for genetic association with vaccine responses in participants enrolled in the phase 1/2 (COV001) and phase 2/3 (COV002) randomized single-blind ChAdOx1 nCoV-19 (AZD1222) vaccine efficacy trials, conducted within the United Kingdom, and in whom humoral immune responses were measured post-vaccination. **Fig. 1** summarises participant inclusion. DNA from 1,222 ChAdOx1 nCoV-19 trial participants was genotyped on the Affymetrix AxiomTM HGCoV2 1 array. After quality control (Methods), 667,496 variants in 1,190 individuals were available for single nucleotide polymorphism variant (SNP) imputation (**Supplementary Fig. 1**). Following imputation, 9,325,058 high quality SNPs were tested for association with normalised antibody responses against S and RBD (**Extended Data Fig. 1**) in 1,076 of the 1190 genotyped individuals who had received ChAdOx1 nCoV-19 vaccine, with antibody measures available at 28 days following first vaccination (baseline demographics are shown in **Table 1**). We performed the association analysis adjusting for age, sex, prior SARS-CoV-2 exposure based on anti-nucleocapsid (anti-N) IgG concentrations (N=128, 11.9%), and antibody assay type (all as fixed-effect covariates), for all individuals irrespective of ancestry (**Extended Data Fig. 2**) including a genetic relatedness matrix as a random effect covariate. The mixed model regression analysis

revealed genome-wide significant associations ( $P < 5 \times 10^{-8}$ ) for both anti-S (index variant rs9271374,  $P = 2.6 \times 10^{-8}$ , beta -0.14, SE 0.03) and anti-RBD (rs1130456,  $P = 4.4 \times 10^{-10}$ , beta -0.26, SE 0.04) IgG antibody levels. rs9271374 and rs1130456 are SNPs located within 10 kilobases (kb) of *HLA-DQ* genes (**Fig. 2**) and in linkage disequilibrium (LD) within our multi-ancestry cohort ( $r^2 = 0.65$ ). The distribution of  $P$ -values (**Extended Data Fig. 3A**) and beta coefficients (**Extended Data Fig. 3B**) for all genotyped and imputed variants across this locus show a clear correlation in genetic architecture between these two antibody responses (Spearman's rho coefficient 0.90 and 0.93 for  $P$ -values and beta coefficients respectively) correlated through LD (measured through  $r^2$ ).

These genetic association signals may be falsely observed as a result of two important factors. Firstly, although every effort was made to normalise the antibody levels whilst acknowledging the different platforms for antibody measurement, the final distributions still deviated from normality, which could increase the risk of detecting a genetic association signal by chance (**Extended Data Fig. 1**). Therefore, we performed a further round of inverse normal transformation on the pooled RBD-specific antibody distributions (**Extended Data Fig. 1F**) to create a merged, normalised distribution (**Extended Data Fig. 4A**) and reran the association analysis for anti-RBD antibodies. The rs1130456 association was still present and the most significant association ( $P = 4.7 \times 10^{-9}$ , **Extended Data Fig. 4B-D**). Secondly, given the diverse ancestry of individuals included, it is possible that the association could be a result of confounding due to population structure. The genomic inflation factor ( $\lambda$ ) from our primary RBD association analysis was 1.023. When the extended MHC region was excluded,  $\lambda$  was 1.007 suggesting much of the observed inflation was a result of the large number of variants associated with MHC (**Extended Data Fig. 5A** for Manhattan and **5B** for QQ). Furthermore, given the low levels of natural exposure to SARS-CoV-2 in our population at the time of sampling early in the pandemic, we used our data for anti-N IgG concentrations to again test for excessive inflation using N as a negative control. No associations of genome-wide significance were observed and  $\lambda$  was estimated at 1.017 (**Extended Data Fig. 5C-D**). To further explore the effect of population structure we re-ran our association analyses for RBD including the first ten genetic principal components (PCs)

(derived from the entire genotyped dataset) as additional fixed effect covariates using our mixed-model approach (**Extended Data Fig. 5E-F**).  $\lambda$  using this approach was 0.985, suggesting a degree of overfitting, but again the same variant (rs1130456) remained most significantly associated with RBD-specific antibodies, albeit with a marginally attenuated  $P$ -value ( $1.3 \times 10^{-9}$ ), as to be expected when including multiple additional covariates in the model.

#### HLA imputation and fine-mapping of associated variants

We proceeded to test for evidence of association with S- and RBD-specific IgG antibodies at the level of HLA gene and protein variation. Imputation (see Methods) identified 640 HLA alleles and 4513 amino acid (AA) changes (of which 81 alleles and 3027 AA substitutions were present in our dataset at a minor allele frequency of  $\geq 0.05$ ). To undertake fine-mapping we identified 1,023 individuals with identity-by-descent (IBD) values of 0.185 or less, and those of self-reported, and PC analysis (PCA)-derived European ancestry (using PC1 and PC2 cut-offs as shown in **Extended Data Fig. 2** inset). Of all HLA and AA alleles tested for association with S and RBD antibody levels, the HLA allele with the most significant association was HLA-DQB1\*06 with anti-RBD antibodies ( $P=3.2 \times 10^{-9}$ , beta 0.27, SE 0.04; **Supplementary Table 1**). An AA variant had a  $P$ -value identical to that of HLA-DQB1\*06 ( $3.2 \times 10^{-9}$ ), but the exact inverse beta coefficient ( $-0.27$ ). This AA variant (DQB1-125A/S) denotes the presence of either an alanine or serine at position 125 of the HLA-DQB1 protein according to international ImmunoGeneTics project (IMGT) coordinates. HLA-DQB1\*06 has a glycine at position 125 whereas other alleles common in our genotyped population possess either alanine (HLA-DQB1\*02 and \*04 alleles) or serine (HLA-DQB1\*05). Thus, this AA variant is synonymous with the presence of HLA-DQB1\*06 in our dataset. The index-associated variant from the primary analysis (rs1130456) was equally associated with the anti-RBD titres in this analysis (beta 0.27, se 0.04). Other variants imputed using the specific HLA imputation algorithm were identified as being marginally more significantly associated than rs1130456, with the new lead being rs9273817 ( $P=2.4 \times 10^{-9}$ , beta=0.27, SE 0.04).

158 To further understand the relationship between the top associated variants we performed stepwise  
 159 forward regression analysis incorporating the full set of SNP, AA and HLA allele variants from HLA  
 160 imputation in the set of individuals restricted by IBD, PCs and self-reported ethnicity (**Fig. 3A and B**).  
 161 Adjusting for the new top SNP (rs9273817) in the first round of conditional analysis, there was a  
 162 complete abolition of the signals for both rs1130456 ( $P=0.65$ ) and HLA-DQB1\*06 ( $P=0.65$ ),  
 163 supporting the likelihood that these variants are all tagging the causal variant, most plausibly HLA-  
 164 DQB1\*06 (**Fig. 3A and 3B** middle rows). A second, likely independent, signal of association was  
 165 observed in HLA-DRB1 with the index variant being the presence of a glutamate or arginine at  
 166 position 71 (according to IMGT) of HLA-DRB1 (DRB1-71E/R,  $P_{\text{conditional}}=2.7 \times 10^{-4}$ ,  $\beta=-0.14$ ,  $SE=0.04$ ,  
 167 **Fig. 3A** middle row). After conditioning on this variant no further independent signals with a  $P < 1 \times 10^{-2}$   
 168 were observed in the class II MHC region. Before proceeding with further fine-mapping, we  
 169 confirmed that both the HLA-DQB1\*06 and DRB1-71E/R associations were robust to statistical  
 170 inflation by performing a Monte Carlo exact test with  $10^8$  permutations. The likelihood of both  
 171 associations occurring by chance was still less than the number of permutations (i.e.,  $P < 2 \times 10^{-8}$ )  
 172 limited only by computational time for testing. Furthermore, we tested for evidence of both the  
 173 HLA-DQB1\*06 and DRB1-71E/R associations in the different population strata (including 928  
 174 European vs 148 non-European) individuals and observed evidence of the same trend of association  
 175 in both groups supporting further that this association is unlikely to be spurious due to population  
 176 structure (**Supplementary Fig. 2**).  
 177 Given our findings from the stepwise conditional analysis we next sought evidence to further  
 178 substantiate the effect being driven by the DQ locus and the relationship of the two independent  
 179 associations to each other. Firstly, HLA-DQB1\*06 is frequently inherited as part of a common  
 180 haplotype with HLA-DQA1\*01 (with DQA1\*01:02 being associated with anti-RBD antibody levels in  
 181 our discovery dataset with a  $P=1.3 \times 10^{-8}$ ,  $\beta=0.28$ ,  $SE=0.05$ ) and HLA-DRB1\*15 (DRB1\*15:01  
 182  $P=1.8 \times 10^{-8}$ ,  $\beta=0.31$ ,  $SE=0.05$ ). These three alleles were most significantly associated with anti-spike  
 183 antibody levels ( $P=2.0 \times 10^{-7}$ ,  $7.8 \times 10^{-8}$  and  $4.6 \times 10^{-8}$  respectively; **Supplementary Table 2**). We assessed

the accuracy of HLA allele imputation by analysing 60 individuals from the genotyped COV001 and COV002 vaccinees (120 alleles) who also underwent classical HLA typing (**Supplementary Notes**). The agreement between 2-digit calls was 99.2% and 96.7% for HLA-DQB1 and HLA-DRB1 loci respectively (**Supplementary Table 3**). The accuracy of calling the specific HLA-DQB1\*06 group of alleles to 4-digit resolution was 97.0%, and 100% for HLA-DRB1\*15 alleles (**Supplementary Table 4**).

In order to confirm that the HLA-DQB1\*06 allele was the most likely primary gene locus associated with the antibody response, we used Bayesian Information Criterion modelling with phased data. We found variation in RBD antibody levels was best described using HLA-DQ alleles (HLA-DQA1\*01/HLA-DQB1\*06, BIC 2715.2) rather than HLA-DRB1 (HLA-DRB1\*15, BIC 2719.1) supporting that the primary association was likely linked to HLA-DQ, rather than HLA-DR, variation (**Supplementary Fig. 3**). We next investigated whether there was evidence of interaction between the HLA-DQB1\*06 and independent DRB1-71E/R associations. Using a likelihood ratio test (LRT) comparing the linear and interaction terms we found no evidence of a complex inter-dependence between these two variants ( $P=0.44$ , **Supplementary Fig. 4**). We therefore compared models describing variation in a simple linear additive model (i.e. normalised anti-RBD antibody levels  $\sim$  HLA-DQB1\*06 + DRB1-71E/R) compared with a model where we compared individuals grouped into the presence of one variant in the absence of the other (**Fig. 3C**) and found that the latter was more parsimonious after adjusting for age, sex, 5 PCs and anti-RBD antibody measurement assay (BIC 2965.42 vs 2689.65 respectively). Thus, using this combined description of variation we next tested for association of HLA-DQB1\*06 with increased anti-RBD antibody levels accounting for DRB1-71E/R over the time course of the ChAdOx1 nCoV-19 trial. We found significant differences between the opposing DQB1\*06 and DRB1-71E/R carrier groups seen at day of second dose ( $P=2.7 \times 10^{-7}$  using the Student's t-test), day 28 post-second dose ( $P=2.6 \times 10^{-7}$ ) and at day 90 post-second dose ( $P=0.01$ , **Fig. 4A**). There was no significant difference observed at day 182 post-second dose. A summary of the baseline demographics of individuals stratified by HLA allele group is provided in **Supplementary Table 5**.

## Replication of genetic association signals with COVID-19 vaccination antibody responses

In order to provide further evidence that the observed genetic associations were robust and not restricted to the COV001 and COV002 cohorts, we aimed to test for replication of the associations in a series of independently recruited cohorts (**Extended Data Fig. 6**). Three trials were coordinated after COV001 and COV002 to address questions regarding safety and immunogenicity of heterologous dosing of COVID-19 vaccines (COMCOV, COMCOV2) and to assess immunogenicity and safety in children (COV006). DNA from 1,722 individuals (638 COMCOV, 876 COMCOV2 and 208 COV006) were genotyped on the same Affymetrix Axiom™ HGCoV2 1 array with identical QC and imputation pipelines applied as to the COV001 and COV002 cohorts. After quality control, data from 1,677 (627 COMCOV, 847 COMCOV2 and 203 COV006) individuals were available (**Supplementary Table 6**). These replication cohorts differed substantially from the ChAdOx1 nCoV-19 trials in respect to age, sex proportions, and timing and nature of vaccination regimens and only data for S antibody levels (and not RBD) were available. Moreover, COMCOV was enriched for non-White reported ethnicities. Nevertheless, when using the same HLA-DQB1\*06 and DRB1-71E/R classifications, we observed statistical evidence of association with anti-S antibody levels measured at the time of second vaccination in the same direction as observed for COV001 and COV002 when looking both at those individuals receiving ChAdOx1 nCoV-19 or BNT162b2 as their first vaccine. Both unadjusted and adjusted models were used to compare the groups as follows.

When including all individuals irrespective of the first vaccine received (all individuals genotyped from COMCOV, COMCOV2 and COV006 received either ChAdOx1 nCoV-19 or BNT162b2 as their first vaccine), there was a significant difference in anti-S antibody levels measured on the day of second vaccine (median of 67 days with a range of 28-184 days following the first vaccine) when comparing the group “carrying DRB1-71E/R with no DQB1\*06” against both those “carrying DQB1\*06 with no DRB1-71E/R” ( $P_t=5.4 \times 10^{-3}$ ;  $P$ -value derived from the t-test), and the “remainder” of individuals ( $P_t=0.02$ , **Supplementary Fig. 5A**). Significant differences in anti-S antibody levels were also observed

for those individuals given a first dose of BNT162b2 comparing the groups “carrying DRB1-71E/R with no DQB1\*06” and those “carrying DQB1\*06 with no DRB1-71E/R” ( $P_t=0.01$ ), and the “remainder” of individuals ( $P_t=0.04$ , **Supplementary Fig. 5B**), and for ChAdOx1 nCoV-19 with significance only observed for the comparison between “Carrying DRB1-71E/R with no DQB1\*06” and “Carrying DQB1\*06 with no DRB1-71E/R” groups ( $P_t=0.04$ , **Supplementary Fig. 5C**). Using a linear model adjusting for age, sex, interval between vaccination and sampling, first vaccine, study and self-reported ethnicity there was a significant difference in S antibody levels observed for all individuals when testing the effect of HLA-DQB1\*06 accounting for DRB1-71E/R ( $P_{LRT}=5.2 \times 10^{-3}$  using the LRT to compare with the null), and for those individuals primed with BNT162b2 ( $P_{LRT}=0.02$ ), with a trend towards significance for individuals primed with ChAdOx1 nCoV-19 ( $P_{LRT}=0.1$ ). Similarly, we observed a significant effect in the same direction when performing the same analysis comparing individuals grouped by either HLA-DQB1\*06 carriage alone ( $P_{LRT}=0.04$ ) or DRB1-71E/R carriage alone ( $P_{LRT}=7.8 \times 10^{-4}$ ). All together, we have found further evidence that carriage of HLA-DQB1\*06 and the presence of either a glutamate or arginine at position 71 in the HLA-DRB1 protein is associated with differential antibody responses to S across individuals, irrespective of the nature of first vaccine, and across ages and both self-reported White and non-White ethnicities. Given the correlation in antibody levels against S and RBD in our discovery set, it is likely that our observed genetic signal would also be observed for RBD even though RND was not measured directly in the replication cohorts.

#### Testing for association of genetic variants on immune response over time and risk of breakthrough infection

Given the observed association between HLA variants with variable immunogenicity, we next investigated whether there was a relationship with risk of breakthrough infection. At a median of 494 days (interquartile range (IQR) 479-535) of follow-up from the first dose of vaccine in participants from the trials used in the discovery analysis (COV001 and COV002), 112 episodes of breakthrough infection (individuals with a SARS-CoV-2 nucleic acid amplification test (NAAT)-positive

262 swab at least 22 days after a first dose of vaccine, with the prevalent ancestral virus and Alpha  
 263 variants) had been recorded in genotyped individuals who had received the ChAdOx1 nCoV-19  
 264 vaccine (**Table 1** and **Supplementary Table 7**). We found that HLA-DQB1\*06 was present in 33.9% of  
 265 individuals experiencing breakthrough infection compared with 45.6% of those who did not have  
 266 breakthrough infection ( $\chi^2 P=0.02$ ). We subsequently found that individuals carrying HLA-DQB1\*06  
 267 alleles were less likely to experience breakthrough infection over time compared with those who did  
 268 not carry HLA-DQB1\*06 after adjustment for age, sex, the first two genetic PCs (representing  
 269 ethnicity), healthcare worker status, BMI and chronic disease status (adjusted HR 0.63, 0.42-0.93,  
 270  $P=0.02$ , **Fig. 4B** and **Extended Data Fig. 7**). We performed sample re-weighting for dose and interval  
 271 between first and second dose of vaccination (using inverse probability weighting) to ensure our  
 272 analyses were as consistent with prior correlates analyses as possible<sup>13</sup>. This significance persisted  
 273 even after adjusting for whether individuals were likely to have been naturally exposed to SARS-  
 274 CoV2 (determined using N measurements) and based on whether they were related to each other  
 275 (IBD<0.185) or not ( $P=0.02$ ). A similar effect was observed when describing individuals using our  
 276 overall HLA status definition (i.e., carrying HLA-DQB1\*06 alleles accounting for DRB1-71E/R),  
 277 although significance was lost (adjusted HR for the group “carrying DRB1\*06 with no DRB1-71E/R”  
 278 0.54, 0.26-1.1,  $P=0.09$ ; **Fig. 4C** and **Extended Data Fig. 8**). The lower frequency of HLA-DQB1\*06 in  
 279 individuals experiencing breakthrough infection was observed both in the 41 individuals meeting the  
 280 definition of primary symptomatic breakthrough infection (31.7% carrying HLA-DQB1\*06 amongst  
 281 those with the primary definition of breakthrough infection), and the 66 who were asymptomatic  
 282 (28.8%), but not in the 9 individuals who did not meet the primary definition of symptomatic  
 283 breakthrough (66.7%) (**Supplementary Table 7**). To further substantiate our finding, we explored  
 284 whether we could find any evidence of an equivalent effect in the tested replication cohorts,  
 285 acknowledging that the cohorts differed significantly from ChAdOx1 nCoV-19 not only in regards to  
 286 age, ethnicity, comorbidities and the predominant circulating SARS-CoV-2 variant (Alpha and Delta),  
 287 but also because breakthrough infection was defined through self-report rather than active



surveillance. In the subset of individuals of self-reported White ethnicity and less than or equal to 55 years of age (thus enriching for individuals more representative of the COV001 and COV002 trial, n=401), there were 29 individuals experiencing breakthrough and 372 individuals with no breakthrough reported after a median of 280 days of follow-up (IQR 244-332). HLA-DQB1\*06 was observed in 37.9% of individuals experiencing breakthrough infection and 40.3% in individuals with no breakthrough infection. After adjustment for age, sex, first vaccine received (ChAdOx1 nCoV-19 or BNT162b2), and booster received (viral vector (ChAdOx1 nCoV-19), mRNA (BNT162b2 or mRNA-1273) or nanoparticle (NVXCoV2373)) with reweighting calculated based on days between first and second doses of vaccine, carriage of HLA-DQB1\*06 had an adjusted HR of 0.87 (0.41-1.80, P=0.73) of risk of breakthrough infection (**Extended Data Fig. 9**).

#### Structural insights into HLA-Spike peptide binding

Given the observed immunological and clinical impact of HLA-DQB1\*06 on vaccine response and effectiveness, we next tested for structural evidence of binding of S peptides by the associated HLA-DQB1\*06 allele. We tested the hypothesis that HLA-DQB1\*06:02 could bind peptides from SARS-CoV-2 Spike more effectively than an alternative HLA-DQB1 allele that was both common in the population and linked with another HLA-DQA1\*01 allele. Using the COV001/COV002 data we identified HLA-DQB1\*05:01 as an allele that would act as a suitable comparator (frequency in COV001/COV002 12%, beta for association with 28-day RBD levels -0.14, se 0.05, P=0.01, acknowledged to commonly pair with HLA-DQA1\*01:01<sup>28</sup>). Other HLA alleles that were common in our merged COV001/COV002 dataset were less suitable for this analysis. DQB1\*03, for example, (frequency 34%) pairs more frequently with DQA1\*03 or \*05 alleles, whereas DQB1\*02 (23%) pairs with DQA1\*02 or \*05). The only available crystal structure for DQB1\*06 alleles is the HLA-DQA1\*01:02-HLA-DQB1\*06:02 in complex with a hypocretin peptide (LPSTKVSAAV)<sup>29</sup>. The key side chains of Ser (position (P) 3), Thr (P4) and Val (P6) of the peptide are buried in the centre of the groove formed by two HLA molecules (**Extended Data Fig. 10A**). Thus, we searched for a hypocretin-like peptide motif (Ser/Cys) ThrXVal in Spike protein (where X is any amino acid with its side chain

pointing away from the groove; Ser and Cys differ in one atom only). Spike residues Val615-NCTEVPVAI-His625 could be aligned with a hypocretin peptide and thus enabled us to model a complex of HLA-DQA1\*01:02–HLA-DQB1\*06:02 bound to the Spike peptide using AlphaFold<sup>30</sup> (**Fig. 5A**). Both the AlphaFold-based model and the crystal structure support DQB1\*06:02 interacting differently with any peptide compared with DQB1\*05:01. DQB1\*05:01 differs from DQB1\*06:02 by at least three key residues forming hydrogen bonds with the bound hypocretin peptide (**Extended Data Fig10B-D**), making analogous DQB1\*05:01–peptide interactions impossible. Our analysis identifies specific residues of DQB1\*05:01 and DQB1\*06:02 responsible for different peptide recognition and subsequent recognition by T-cell receptors.

### Immunological implications of the observed MHC associations

To further support these observations, we used peripheral blood mononuclear cells (PBMCs) available from a small number of participants from COV001 and COV002 to compare anti-S specific memory B-cell responses at day 84 following the first vaccine in 10 individuals carrying HLA-DQB1\*06, and 10 not carrying HLA-DQB1\*06. We observed an increase in anti-S memory B-cell responses in the individuals carrying HLA-DQB1\*06 ( $P=0.05$  using a one-tailed Wilcoxon-rank test) at Day 84 that was not apparent at Day 0 (**Fig. 5B**). We then searched for similar signals of association in the intermediate components of the MHC-T-B-antibody axis. We observed a difference in overall CD4 proliferation in response to stimulation with S1 (that includes the RBD domain and the putative Val615-NCTEVPVAI-His625 peptide,  $P=0.01$  **Fig. 5C**), but not against S2 (cleaved away before residue 686). We did not observe an equivalent signal with antigen specific T-cell activation (using the antigen inducible marker (AIM) assay, **Fig. 5D**).

### Discussion

Our findings show that individuals carrying HLA-DQB1\*06 alleles have higher antibody responses against SARS-CoV-2 spike protein and the RBD following vaccination with both ChAdOx1 nCoV-19 and BNT162b2 vaccines than individuals not carrying this allele. HLA-DQB1\*06 is also associated with a reduced risk of breakthrough infection based on PCR positivity after a median 494 days of follow

up after receiving their first dose of vaccine. To our knowledge, this is the first report of an HLA association with antibody responses following immunisation with SARS-CoV-2 vaccines and of a genetic association with risk of SARS-CoV-2 breakthrough infection<sup>15–18,22–24,31</sup>. We further provide a working mechanistic hypothesis for the primary HLA-DQB1\*06 association of potentially distinct peptide binding that may lead to improved CD4+ T-cell proliferation and memory B-cell activation. Our study design comprised of an infection- and vaccine-naïve population in a clinical trial setting with appropriate blinding, detailed immune phenotyping and patient follow up at defined timepoints, and we further substantiated our findings in a large replication dataset with preliminary follow-up functional experiments.

The global evidence of breakthrough infections following vaccination, of changes in immune correlates of protection over time, and of new SARS-CoV-2 variants highlight the importance of subsequent dosing of vaccination and understanding how this can be optimally deployed.<sup>9,13,32</sup> Our study demonstrates that there is a heritable component to observed inter-individual variation in antibody response at day 28 post-first dose but also throughout time post-vaccination, across vaccinee age and type of first vaccine. Given that these effects do persist over time, with some change in effect size, and have clinical relevance in terms of risk of breakthrough infection, the observed HLA associations raise the potential utility of prioritising at-risk populations based, for example, on HLA-DQB1\*06 allele frequencies, among whom more intensive booster vaccination may be warranted. Variable HLA-DQB1\*06 allele frequencies are reported across diverse populations<sup>33,34</sup> but there is not yet robust epidemiological evidence of the extent of breakthrough infections in such populations and this would require further investigation before implementation of such an intervention. The observed reduction in effect size on log10 transformed RBD-specific antibody levels in the ChAdOx1 nCoV-19 vaccinees over time from 0.38 at day 28, to 0.32 at boost, 0.17 at day 28 post-boost and 0.12 at day 90 may represent a true reduction in effect of genetic variation over time, or could also be a result of the limit of detection and dynamic range of the antibody assay.

Further re-analyses using recalibrated assay detection systems would be necessary to resolve this issue.

Although we have provided preliminary evidence for our mechanistic hypothesis for HLA-DQB1\*06, further studies to understand the structure-function relationships based on the specific allele/peptide predictions and T cell biology will be required. Previous genetic studies for non-SARS-CoV-2 vaccines implicating the MHC suggest both HLA-peptide binding<sup>23,37</sup> and non-HLA effects relating, for example, to differential gene expression or complement activation<sup>24</sup>, as potential underlying mechanisms for observed genetic associations. For SARS-CoV-2 vaccine response, consideration of HLA genotype has been advocated in vaccine design based on predicted antigens presented to T cells across different ethnic groups in order to maximise efficacy based on T cell immunity, with potential utility as a booster agent to strengthen immune responses<sup>38</sup>.

Limitations of the study include the need for further replication of the genetic association in other studies and populations, and the representativeness of the trial population to the wider UK and global population. We propose that there is an urgent need to investigate these associations further in diverse ethnic groups and individuals of varying comorbidity to maximise insights and potential utility of the observed associations. There is also a requirement for mechanistic studies to further understand the functional basis of the association, and the relationship with specific SARS-CoV-2 variants. A further limitation is the extent to which fine mapping the association to specific variants and modulated genes was possible, reflecting the high level of sequence and structural polymorphism, sequence homologies and complex LD in the MHC<sup>39</sup>. Only two antibody responses were analysed, with a greater antibody repertoire and T cell immune response assays and other aspects of cell mediated immunity important to include in future studies.

We propose that to inform vaccine design and implementation against COVID-19 and other vaccine-preventable diseases with products either established or in development, an understanding of the

impact of human genetics should be prioritised to deliver translational outputs for the long-term benefit of populations world-wide.

## Acknowledgements

The study is funded by the University of Oxford COVID-19 Research Response Fund and UK Research and Innovation. The ChAdOx1 nCoV-19 (AZD1222) vaccine efficacy trials were funded by the UK National Institute for Health Research, UK Research and Innovation, the Bill & Melinda Gates Foundation, the Lemann Foundation, Rede D'OR, the Brava and Telles Foundation, and the South African Medical Research Council. The views expressed are those of the authors and not necessarily those of the NIHR or the Department of Health and Social Care. The authors are grateful to the volunteers who participated in this study. AstraZeneca reviewed the data from the study and the final manuscript prior to submission, but the authors retained editorial control. JCK is supported by a Wellcome Trust Investigator Award (grant number 204969/Z/16/Z) and the NIHR Oxford Biomedical Research Centre. AJM is an NIHR Academic Clinical Lecturer. The research was supported by the Wellcome Trust Core Award Grant Number 203141/Z/16/Z with additional support from the NIHR Oxford BRC and an Academy of Medical Sciences Starter Grants awarded to AJM (SGL024\1096)

## Author contributions

Conceptualisation (JCK, DOC, AJM, AJP, TL), data curation (AJM, DOC), formal analysis (AJM, DOC), funding acquisition (JCK, AJP), investigation (DOC, AJM, JCK, TL, SB, IC, EAC, TDe, TDi, NJE, SF, SF, ALF, EKT, GL, XL, NM, LG, RM, MBB, JF, BA, TM, AYC, KS, RHS, MV), project administration (JCK, AJP, TL), supervision (JCK, AJP, TL), validation (AJM, DOC, JCK), visualisation (AJM, DOC, JCK), writing – original draft (JCK, AJM, DOC, AJP, TL), and writing – review & editing (JCK, AJM, DOC, AJP, TL, SF, MV). All authors critically reviewed and approved the final version.

## Ethics declarations

### Competing Interests

The University of Oxford has entered into a partnership with AstraZeneca for further development of ChAdOx1 nCoV-19. TL is named as an inventor on a patent application covering this SARS-CoV-2 vaccine and was a consultant to Vaccitech for an unrelated project. AJP is Chair of the UK DHSC Joint Committee on Vaccination & Immunisation but does not participate in discussions on COVID-19 vaccines, and is a member of the Strategic Advisory Group of Experts on Immunization to the WHO (World Health Organization). AJP is an NIHR senior investigator. The remaining authors declare no competing interests. The views expressed in this article do not necessarily represent the views of the DHSC, JCVI, NIHR, or WHO.

## Tables and Figures

Table 1

Baseline characteristics for 1,076 ChAdOx1 nCoV-19 participants in the Phase 1/2 (COV001) and Phase 2/3 (COV002) trials who received ChAdOx1 nCoV-19 vaccine with genotype data available, and for the 1,069 individuals who either experienced a breakthrough infection after 21 days or who did not experience a breakthrough up to time of censoring. Seven individuals were not included in the breakthrough analysis as they experienced breakthrough infection within 22 days of receiving their first vaccine. Statistical differences were tested across groups using  $\chi^2$  tests or exact Fisher tests if any group contained less than 5 observations.

Characteristic (range where applicable)	Genotyped cohort (ChAdOx1 vaccinated) N=1,076	No reported breakthrough infection (N=957)	Breakthrough infection reported (N=112)	Evidence of difference between breakthrough groups (P)
<b>Age at recruitment</b>	37.0 (30.0-47.0)	37.0 (30.0-47.0)	37.0 (28.8-48.0)	NS
18-55yrs, number (%)	1076 (100)	957 (100)	112 (100)	
Missing, number (%)	0 (0)	0 (0)	0 (0)	NS
<b>Sex, number (%)</b>				
Female	572 (53.2)	514 (53.7)	56 (50.0)	
Male	504 (46.8)	443 (46.3)	56 (50.0)	NS
<b>BMI</b>				
Median (IQR)	24.7 (22.6-27.5)	24.7 (22.5-27.5)	25.2 (22.7-28.3)	NS
<b>Ethnic group, number (%)</b>				
White	974 (90.5)	865 (90.4)	102 (91.1)	
Asian	50 (4.7)	44 (4.6)	6 (5.3)	
Black	10 (0.9)	9 (0.9)	1 (0.9)	
Mixed	29 (2.7)	26 (2.7)	3 (2.7)	
Other	13 (1.2)	13 (1.4)	0 (0)	
Not reported / missing	0 (0)	0 (0)	0 (0)	NS
<b>Health and social care setting workers (HCW), number (%)</b>				
Not HCW	590 (54.8)	539 (56.3)	48 (42.9)	
HCW unknown COVID contacts	101 (9.4)	91 (9.5)	10 (8.9)	
HCW with $\leq 1$ COVID contacts	267 (24.8)	226 (23.6)	40 (35.7)	
HCW with $> 1$ COVID contacts	118 (11.0)	101 (10.6)	14 (12.5)	0.02
<b>Comorbidities, number (%)</b>				
Cardiovascular	35 (3.3)	29 (3.0)	6 (5.2)	NS
Respiratory	73 (6.8)	59 (6.1)	14 (12.5)	0.02
Diabetes	9 (0.8)	7 (0.7)	2 (1.8)	NS
<b>Interval between first and second vaccine, number (%)</b>				
$< 6$ weeks	12 (1.1)	11 (1.1)	1 (0.9)	
6-8 weeks	151 (14.0)	133 (13.9)	17 (15.2)	
9-11 weeks	257 (23.9)	220 (23.0)	33 (29.5)	
$\geq 12$ weeks	556 (51.7)	501 (52.4)	53 (47.3)	
none	100 (9.3)	92 (9.6)	8 (7.1)	NS
<b>Vaccines received prior to infection occurring, number (%)</b>				
SD	499 (46.4)	463 (48.4)	35 (31.3)	
SD / SD	400 (37.2)	342 (35.7)	54 (48.2)	
LD / SD	167 (15.5)	143 (15.0)	22 (19.6)	
SD / LD	10 (0.9)	9 (0.9)	1 (0.9)	0.005
<b>HLA carrier, number (%)</b>				
HLA-DQB1*06	474 (44.1)	436 (45.6)	38 (33.9)	0.02
DRB1-71E/R	881 (81.9)	784 (81.9)	92 (82.1)	NS
<b>HLA status, number (%)</b>				
Carrying DRB1-71E/R with no DQB1*06	532 (49.4)	464 (48.5)	63 (56.3)	
Remainder	419 (38.9)	377 (39.4)	40 (35.7)	
Carrying DQB1*06 with no DRB1-71E/R	125 (11.6)	116 (12.1)	9 (8.0)	NS

437

438 [Figure 1](#)

439 Flow diagram of participants selected for analysis from the Phase 1/2 (COV001) and Phase 2/3  
440 (COV002) vaccine trials. For breakthrough infections, symptomatic individuals had primary  
441 symptoms of COVID-19 (cough, shortness of breath, fever, anosmia or ageusia); if they presented  
442 with symptoms other than the five primary COVID-19 symptoms, they were categorised as  
443 nonprimary symptomatic cases.\* samples selected to maintain investigator blinding during sample  
444 selection.

445

ACCELERATED ARTICLE PREVIEW



446

447

448 **Figure 2**

449 Genome-wide and MHC SNP associations with RBD antibody level in 1,076 ChAdOx1 nCoV-19  
450 vaccine recipients from the COV001 and COV002 vaccine trials. The association results for all tested  
451 autosomal and X chromosome variants with linear regression in a mixed-model framework are  
452 shown on the left in a Manhattan plot with the red horizontal line representing the nominal  
453 threshold for GWAS significance ( $P=5 \times 10^{-8}$ ) to account for the multiple tests performed. The QQ plot  
454 in the inset with expected  $P$ -values shown on the X axis and observed on the Y axis. A magnified view  
455 of a portion of the MHC locus is shown on the right of the Figure. All points represent SNPs  
456 positioned by build 37 of the human genome coordinates and coloured on the right by linkage  
457 disequilibrium ( $r^2$ ) with relevant gene coordinates provided on the lower panel.

458

459 **Figure 3**

460 Fine-mapping the likely causal variants associated with day 28 post-prime anti-RBD antibody levels  
461 (normalised within immunoassay performed at MSD and PPD laboratories) in COV001 and COV002.  
462 A) and B) Stepwise conditional analyses using linear regression were performed in 1,023 individuals  
463 restricted by self-reported White ethnicity and PCA axes, and with IBD values less than or equal to  
464 0.185. The primary unconditional association analysis across the class II MHC region (A) and HLA-  
465 DQB1 (B) locus is shown in the top rows with points shaped by variant type (amino acid (AA), HLA  
466 allele (HLA), insertion-deletion (INDEL) or single nucleotide variant (SNP) and coloured by linkage  
467 disequilibrium ( $r^2$ ) with the index variant (rs9273817). The key variants of interest (rs9273817,  
468 rs1130456 and HLA-DQB1\*06) are highlighted. The middle and bottom rows represent the same  
469 points after adjustment for rs9273817 (middle row) and also DRB1-71E/R (bottom row) using the  
470 same shape and colour definitions as the first row. (C) 1,076 individuals from COV001/COV002  
471 grouped by carriage of either DQB1\*06 or DRB1-71E/R in absence of the other demonstrate the  
472 most significant differences between groups tested using the two-sided Student's t-test as shown by  
473 violin plots overlain by box plots. The box plot center line represents the median; the box limits, the  
474 upper and lower quartiles; and the whiskers are the 1.5x interquartile range. \*\*\*  $P < 0.001$ .

475

476 **Figure 4**

477 The effect of HLA-DQB1\*06 on anti-RBD antibody accounting for DRB1-71E/R persists over time and  
478 influences risk of breakthrough infection in COV001 and COV002 in genotyped vaccine recipients. A)  
479 Where PPD-measured anti-RBD antibody levels were available in COV001 and COV002, the  
480 differences in vaccine responses by HLA type persisted over time. Differences were tested between  
481 the categories “Carrying DRB1-71E/R with no DQB1\*06” and “Carrying DQB1\*06 with no DRB1-  
482 71E/R” using the two-tailed Student’s t-test. Times of sampling are either after first or second (post-  
483 boost (PB)) vaccine doses. B) and C) Adjusted Cox regression curves with risk of breakthrough  
484 infection over time in 1,069 individuals stratified by carriage of (B) HLA-DQB1\*06 alleles and (C) HLA-  
485 DQB1\*06 accounting for DRB1-71E/R status in COV001 and COV002 vaccine recipients adjusted for  
486 age, sex, reported ethnicity, healthcare worker status, BMI and chronic disease status and including  
487 sample weighting for dose and interval between prime and boost vaccination. Included individuals  
488 had breakthrough infection at least 22 days after first vaccination. Box plot center line, median; box  
489 limits, upper and lower quartiles; whiskers, 1.5x interquartile range \*\*  $P < 0.01$ ; \*  $P < 0.05$ ; NS not  
490 significant; PB: post-boost.

491  
492  
493  
494  
495  
496

497 **Figure 5**

498 The clinical implications and mechanisms of the HLA associations with differential Spike / RBD  
499 antibody levels. A) AlphaFold-based model of HLA-DQA1:01:02–HLA-DQB1:06:02–Spike peptide. The  
500 peptide is shown in orange. Residue numbering corresponds to UniProt ID P0DTC2. B) Memory B-  
501 cell, C) CD4+ T-cell proliferation and D) antigen inducible marker (AIM) CD4+ T-cell responses using  
502 biologically independent samples from 20 individuals from COV001 and COV002 stratified by  
503 carriage of HLA-DQB1\*06 allele carriage sampled at days 0 and 84 following first vaccine with  
504 significant differences tested for using a one-sided Wilcoxon-rank test. Statistical differences were  
505 seen between HLA carriage groups for the memory B-cell responses (B,  $P=0.05$ ) and S1 proliferation  
506 response (C,  $P=0.01$ ) at day 84. Box plot center line, median; box limits, upper and lower quartiles;  
507 whiskers, 1.5x interquartile range. \*  $P<0.05$ .

508

509

510

## 511 References

- 512 1. COVID-19 Map - Johns Hopkins Coronavirus Resource Center. Available at:  
513 <https://coronavirus.jhu.edu/map.html>. (Accessed: 26th September 2022)
- 514 2. Taylor, L. Covid-19: True global death toll from pandemic is almost 15 million, says WHO. *BMJ*  
515 **377**, o1144 (2022).
- 516 3. Polack, F. Safety and efficacy of the BNT162b2 mRNA COVID-19 vaccine. *N. Engl. J. Med.* **383**,  
517 2603–2615 (2020).
- 518 4. Voysey, M. *et al.* Safety and efficacy of the ChAdOx1 nCoV-19 vaccine (AZD1222) against  
519 SARS-CoV-2: an interim analysis of four randomised controlled trials in Brazil, South Africa,  
520 and the UK. *Lancet* **397**, 99–111 (2021).
- 521 5. Pritchard, E. *et al.* Impact of vaccination on new SARS-CoV-2 infections in the United  
522 Kingdom. *Nat. Med.* 2021 278 **27**, 1370–1378 (2021).
- 523 6. Lopez Bernal, J. *et al.* Effectiveness of Covid-19 Vaccines against the B.1.617.2 (Delta) Variant.  
524 *N. Engl. J. Med.* **385**, 585–594 (2021).
- 525 7. Vasileiou, E. *et al.* Interim findings from first-dose mass COVID-19 vaccination roll-out and  
526 COVID-19 hospital admissions in Scotland: a national prospective cohort study. *Lancet* **397**,  
527 1646–1657 (2021).
- 528 8. Bergwerk, M. *et al.* Covid-19 Breakthrough Infections in Vaccinated Health Care Workers. *N.*  
529 *Engl. J. Med.* **385**, 1474–1484 (2021).
- 530 9. Bar-On, Y. *et al.* Protection of BNT162b2 Vaccine Booster against Covid-19 in Israel. *N. Engl. J.*  
531 *Med.* **385**, 1393–1400 (2021).
- 532 10. Wei, J. *et al.* Antibody responses to SARS-CoV-2 vaccines in 45,965 adults from the general

- 533 population of the United Kingdom. *Nat. Microbiol.* 2021 1–10 (2021). doi:10.1038/s41564-  
534 021-00947-3
- 535 11. Baum, A. *et al.* REGN-COV2 antibodies prevent and treat SARS-CoV-2 infection in rhesus  
536 macaques and hamsters. *Science* **370**, 1110–1115 (2020).
- 537 12. Khoury, D. *et al.* Neutralizing antibody levels are highly predictive of immune protection from  
538 symptomatic SARS-CoV-2 infection. *Nat. Med.* **27**, 1205–1211 (2021).
- 539 13. Feng, S. *et al.* Correlates of protection against symptomatic and asymptomatic SARS-CoV-2  
540 infection. *Nat. Med.* 2021 1–9 (2021). doi:10.1038/s41591-021-01540-1
- 541 14. Collier, D. A. *et al.* Age-related immune response heterogeneity to SARS-CoV-2 vaccine  
542 BNT162b2. *Nat.* 2021 1–6 (2021). doi:10.1038/s41586-021-03739-1
- 543 15. Newport, M. J. *et al.* Genetic regulation of immune responses to vaccines in early life. *Genes*  
544 *Immun.* **5**, 122–129 (2004).
- 545 16. Milich, D. R. & Leroux-Roels, G. G. Immunogenetics of the response to HBsAg vaccination.  
546 *Autoimmun Rev* **2**, 248–257 (2003).
- 547 17. Png, E. *et al.* A genome-wide association study of hepatitis B vaccine response in an  
548 Indonesian population reveals multiple independent risk variants in the HLA region. *Hum.*  
549 *Mol. Genet.* **20**, 3893–3898 (2011).
- 550 18. Zhang, Z. *et al.* Host Genetic Determinants of Hepatitis B Virus Infection. *Front. Genet.* **10**, 696  
551 (2019).
- 552 19. Nishida, N. *et al.* Key HLA-DRB1-DQB1 haplotypes and role of the BTNL2 gene for response to  
553 a hepatitis B vaccine. *Hepatology* **68**, 848–858 (2018).
- 554 20. O'Connor, D. *et al.* Common Genetic Variations Associated with the Persistence of Immunity  
555 following Childhood Immunization. *Cell Rep.* **27**, 3241–3253.e4 (2019).

21. Ovsyannikova, I. G., Pankratz, V. S., Vierkant, R. A., Jacobson, R. M. & Poland, G. A. Consistency of HLA associations between two independent measles vaccine cohorts: a replication study. *Vaccine* **30**, 2146–2152 (2012).
22. Clifford, H. D. *et al.* Polymorphisms in key innate immune genes and their effects on measles vaccine responses and vaccine failure in children from Mozambique. *Vaccine* **30**, 6180–6185 (2012).
23. Suzuki, T., Yamauchi, K., Kuwata, T. & Hayashi, N. Characterization of hepatitis B virus surface antigen-specific CD4+ T cells in hepatitis B vaccine non-responders. *J. Gastroenterol. Hepatol.* **16**, 898–903 (2001).
24. Hohler, T. *et al.* C4A deficiency and nonresponse to hepatitis B vaccination. *J Hepatol* **37**, 387–392 (2002).
25. Mapping the human genetic architecture of COVID-19. *Nat.* **2021** 1–8 (2021). doi:10.1038/s41586-021-03767-x
26. Kousathanas, A. *et al.* Whole-genome sequencing reveals host factors underlying critical COVID-19. *Nat.* **2022** 6077917 **607**, 97–103 (2022).
27. Pairo-Castineira, E. *et al.* Genetic mechanisms of critical illness in COVID-19. *Nat.* **2020** 5917848 **591**, 92–98 (2020).
28. Gonzalez-Galarza, F. F. *et al.* Allele frequency net 2015 update: new features for HLA epitopes, KIR and disease and HLA adverse drug reaction associations. *Nucleic Acids Res* **43**, D784-8 (2015).
29. Siebold, C. *et al.* Crystal structure of HLA-DQ0602 that protects against type 1 diabetes and confers strong susceptibility to narcolepsy. *Proc. Natl. Acad. Sci. U. S. A.* **101**, 1999–2004 (2004).

- 579 30. Jumper, J. *et al.* Highly accurate protein structure prediction with AlphaFold. *Nature* **596**,  
580 583–589 (2021).
- 581 31. Haralambieva, I. H. *et al.* Genome-wide associations of CD46 and IFI44L genetic variants with  
582 neutralizing antibody response to measles vaccine. *Hum Genet* **136**, 421–435 (2017).
- 583 32. Milne, G. *et al.* Does infection with or vaccination against SARS-CoV-2 lead to lasting  
584 immunity? *Lancet Respir. Med.* **0**, (2021).
- 585 33. Gonzalez-Galarza, F. F. *et al.* Allele frequency net database (AFND) 2020 update: gold-  
586 standard data classification, open access genotype data and new query tools. *Nucleic Acids*  
587 *Res.* **48**, D783–D788 (2020).
- 588 34. Hurley, C. *et al.* Common, intermediate and well-documented HLA alleles in world  
589 populations: CIWD version 3.0.0. *HLA* **95**, 516–531 (2020).
- 590 35. Hammer, C. *et al.* Amino acid variation in HLA class II proteins is a major determinant of  
591 humoral response to common viruses. *Am. J. Hum. Genet.* (2015).  
592 doi:10.1016/j.ajhg.2015.09.008
- 593 36. Dendrou, C. A., Petersen, J., Rossjohn, J. & Fugger, L. HLA variation and disease. *Nature*  
594 *Reviews Immunology* **18**, 325–339 (2018).
- 595 37. Nishida, N. *et al.* Importance of HBsAg recognition by HLA molecules as revealed by  
596 responsiveness to different hepatitis B vaccines. *Sci. Rep.* **11**, (2021).
- 597 38. Somogyi, E. *et al.* A Peptide Vaccine Candidate Tailored to Individuals' Genetics Mimics the  
598 Multi-Targeted T Cell Immunity of COVID-19 Convalescent Subjects. *Front. Genet.* **12**, (2021).
- 599 39. Trowsdale, J. & Knight, J. C. Major histocompatibility complex genomics and human disease.  
600 *Annu Rev Genomics Hum Genet* **14**, 301–323 (2013).
- 601 40. Folegatti, P. M. *et al.* Safety and immunogenicity of the ChAdOx1 nCoV-19 vaccine against



- 602 SARS-CoV-2: a preliminary report of a phase 1/2, single-blind, randomised controlled trial.  
603 *Lancet* **396**, 467–478 (2020).
- 604 41. Li, G. *et al.* Safety and immunogenicity of the ChAdOx1 nCoV-19 (AZD1222) vaccine in  
605 children aged 6-17 years: a preliminary report of COV006, a phase 2 single-blind, randomised,  
606 controlled trial. *Lancet (London, England)* **399**, 2212–2225 (2022).
- 607 42. Stuart, A. S. V. *et al.* Immunogenicity, safety, and reactogenicity of heterologous COVID-19  
608 primary vaccination incorporating mRNA, viral-vector, and protein-adjuvant vaccines in the  
609 UK (Com-COV2): a single-blind, randomised, phase 2, non-inferiority trial. *Lancet (London,*  
610 *England)* **399**, 36–49 (2022).
- 611 43. Liu, X. *et al.* Safety and immunogenicity of heterologous versus homologous prime-boost  
612 schedules with an adenoviral vectored and mRNA COVID-19 vaccine (Com-COV): a single-  
613 blind, randomised, non-inferiority trial. *Lancet (London, England)* **398**, 856–869 (2021).
- 614 44. Purcell, S. *et al.* PLINK: a tool set for whole-genome association and population-based linkage  
615 analyses. *Am J Hum Genet* **81**, 559–575 (2007).
- 616 45. McCarthy, S. *et al.* A reference panel of 64,976 haplotypes for genotype imputation. *Nat*  
617 *Genet* **48**, 1279–1283 (2016).
- 618 46. Luo, Y. *et al.* A high-resolution HLA reference panel capturing global population diversity  
619 enables multi-ancestry fine-mapping in HIV host response. *Nat. Genet.* **53**, 1504–1516 (2021).
- 620 47. Stephens, M., Smith, N. & Donnelly, P. A new statistical method for haplotype reconstruction  
621 from population data. *Am. J. Hum. Genet.* **68**, 978–989 (2001).
- 622 48. Mirdita, M. *et al.* ColabFold: making protein folding accessible to all. *Nat. Methods* **19**, 679–  
623 682 (2022).
- 624 49. Trück, J. *et al.* The zwitterionic type I *Streptococcus pneumoniae* polysaccharide does not

- 625 induce memory B cell formation in humans. *Immunobiology* **218**, 368–372 (2013).
- 626 50. Clutterbuck, E. A. *et al.* Serotype-specific and age-dependent generation of pneumococcal  
627 polysaccharide-specific memory B-cell and antibody responses to immunization with a  
628 pneumococcal conjugate vaccine. *Clin. Vaccine Immunol.* **15**, 182–193 (2008).
- 629 51. Yang, J., Lee, S. H., Goddard, M. E. & Visscher, P. M. GCTA: a tool for genome-wide complex  
630 trait analysis. *Am J Hum Genet* **88**, 76–82 (2011).
- 631 52. Fay, M. P. & Shaw, P. A. Exact and Asymptotic Weighted Logrank Tests for Interval Censored  
632 Data: The interval R Package. *J. Stat. Softw.* **36**, 1–34 (2010).
- 633 53. Therneau, T. M. & Grambsch, P. M. A Package for Survival Analysis in S, version 2.38. *Model.*  
634 *Surviv. Data Extending Cox Model* (2000).
- 635 54. van der Wal, W. M. & Geskus, R. B. ipw: An R Package for Inverse Probability Weighting. *J.*  
636 *Stat. Softw.* **43**, 1–23 (2011).
- 637 55. Aulchenko, Y. S., Ripke, S., Isaacs, A. & van Duijn, C. M. GenABEL: an R library for genome-  
638 wide association analysis. *Bioinformatics* **23**, 1294–1296 (2007).
- 639
- 640

## Methods

### Study design and participants

#### Discovery cohort

The participants were enrolled in phase 1/2 (COV001) or phase 2/3 (COV002) randomized single-blind ChAdOx1 nCoV-19 (AZD1222) vaccine multi-centre efficacy trials conducted across multiple sites within the United Kingdom<sup>4,40</sup> (NCT04324606, NCT04400838). In brief, following written informed consent, adults aged 18 years and older were randomly assigned to receive either intramuscular ChAdOx1 nCoV-19 (AZD1222) or a control vaccine (MenACWY), to assess the safety and efficacy of the ChAdOx1 nCoV-19 vaccine against SARS-CoV-2<sup>4,40</sup>. All individuals included in the analyses agreed to being included in genetic studies as part of the vaccine trial consent, with the opportunity to opt out. The trials were conducted according to the principles of Good Clinical Practice and approved by the South Central Berkshire Research Ethics Committee (20/SC/0145 and 20/SC/0179) and the UK regulatory agency (the Medicines and Healthcare products Regulatory Agency). Individuals with humoral immune responses measured post-vaccination were selected for this genotyping study. To maintain blinding of investigators to vaccine allocation — prior to vaccine trial reporting — participants who received the control vaccine were also genotyped, at a ratio of 1:10.

**Breakthrough infections.** Participants received weekly reminders to report any primary symptoms of COVID-19 (cough, shortness of breath, fever, anosmia or ageusia), and if symptomatic a SARS-CoV-2 nucleic acid amplification test (NAAT) was performed on a nose and throat swab. Participants were also asked to return a weekly nose and throat swab for NAAT for the duration of the study. A breakthrough infection was defined as SARS-CoV-2 NAAT-positive swab at least 22 days after a first dose of vaccine. If participants were NAAT-positive but had symptoms other than the five primary COVID-19 described above, they were categorised as nonprimary symptomatic cases but still included in the final breakthrough analyses reported herein.

#### Replication cohort

The replication cohort was comprised of participants from three COVID-19 vaccine trials conducted across several sites within the United Kingdom<sup>41–43</sup>. Two of these trials (COMCOV and COMCOV2) were in adults aged 50 years and older, randomised to receive homologous or heterologous two-dose schedules of either intramuscular ChAdOx1 nCoV-19, mRNA vaccines (BNT162b2 or mRNA-1273) or a nanoparticle vaccine (NVX-CoV2373)<sup>42,43</sup>. The other trial (COV006) was in children aged 6–17 who were randomised to receive either intramuscular ChAdOx1 nCoV-19 or a control vaccine (capsular group B meningococcal vaccine, 4CMenB)<sup>41</sup>. All participants included in this manuscript consented (or their parents/guardians) to being included in genetic studies as part of the vaccine trial consent, with the opportunity to opt out in the consent form.

**Breakthrough infections.** Adult participants in the replication cohort self-reported breakthrough COVID-19 (no active COVID-19 testing as part of study) and associated symptoms. Parents/guardians reported PCR-confirmed or lateral flow assay-confirmed SARS-CoV-2 infections for the childhood participants. We defined a breakthrough infection for this cohort as a self-reported case of COVID-19 at least 22 days after a first dose of vaccine.

#### Antibody concentrations

##### Discovery cohort

Blood samples for serological testing were taken at baseline, day 28 after the first dose of vaccine, prior to the second vaccine, and then at day 28, 90 and 182 after the second dose of vaccine. Day 28 post-first vaccine responses were available on all participants, and the variance of response across the cohort was substantial and together this influenced the choice for the discovery GWAS. Humoral immune responses were assessed using Meso Scale Discovery (MSD) multiplexed immunoassay against SARS-CoV-2 S and RBD as well as the nucleocapsid (N) proteins — in the entire phase 1/2 UK cohort (n= 585) and 15% of the phase 2/3 UK cohort (n=637). Sample selection from the phase 2/3 trial was based on samples processed for the initial application for emergency use, which required 15% of samples included in the efficacy trial to be processed on validated assays. In addition,

serological testing was also performed on samples from NAAT-positive individuals — missing data were assumed to be missing at random.

Anti- S, RBD and N IgG levels were measured by a multiplex immunoassay using the MSD platforms at two laboratories; the phase 1/2 samples were performed at MSD and the phase 2/3 samples were performed at PPD Laboratories. Ninety-seven samples were assessed by both laboratories, to evaluate inter-assay agreement.

#### Replication cohort

The replication cohort had blood samples for serological testing taken at baseline participation in the study, which was 28–84 days following the first dose of vaccine and on the day of receiving the second dose of vaccine. Adult participants in the replication cohort had their SARS-CoV-2 anti-S IgG levels measured by enzyme-linked immunosorbent assay (ELISA) at Nexelis (Laval, Canada). In the childhood replication study, anti- S IgG levels were measured using MSD at PPD Laboratories prior to receipt of any further vaccine dose.

#### DNA extraction

DNA was extracted from either blood clots remaining following serum separation by centrifugation or whole blood collected in EDTA tubes. In brief, clots were dispersed by centrifugation through clots spin baskets (Qiagen, catalogue No. 158932). ATL buffer (Qiagen, catalogue No. 1014758) was added to the centrifuged clot and vortexed. Proteinase K (Qiagen, catalogue No. 19131) was added, vortexed thoroughly and incubated in shaking incubator at 56°C until clot was completely lysed (overnight). Following lysis, AL buffer was added (Qiagen, catalogue No. 1038826) and vortexed thoroughly. Lysate or whole blood was then transferred to the QIAasympy 2.0 and extracted using the QIAasympy DSP DNA Midi kit (Qiagen, catalogue No 937255).

#### Genotyping

Standardised DNA was sent to the National Institute for Health Research UK BioCentre and genotyped using their established pipelines on the Affymetrix Axiom™ HGCoV2 1 array. Raw CEL

files were transferred back to Oxford for file conversion into build 38 using the Axiom Analysis Suite Best Practice Workflow. Individual samples and single nucleotide polymorphism (SNP) variants were exported and underwent further quality control using PLINK<sup>44</sup> (version 1.9).

Individuals were excluded if more than 3% of SNPs were classed as missing, or if derived genetic sex did not match reported sex, or if levels of heterozygosity lay more than 3 times the standard deviation from the mean of individuals stratified by self-reported ethnicity. Identity by descent (IBD) was calculated for all pairs of individuals and individuals were excluded if they had estimates  $\geq 0.9$ , excluding the individual with the highest SNP missingness rate from each pair preferentially. Hardy-Weinberg estimates were calculated for each SNP within individuals classified as founders (with  $IBD < 0.05$ ) and SNPs were excluded if exhibiting extreme deviations from equilibrium (using a threshold of  $P < 1 \times 10^{-50}$  calculated in PLINK 1.9).

Principal components were calculated for all individuals both within the genotyped COVID-19 vaccine cohorts and merged with individuals from the 1000 Genomes project derived from Great Britain (GBR), Han individuals from China (CHS) and African individuals from Kenya (LWK) and Nigeria (YRI). Before merging vaccinee data with 1000 Genomes individuals, SNPs were first lifted over from Build 38 to Build 37 coordinates using LiftOver <https://genome.sph.umich.edu/wiki/LiftOver>. Plots were inspected to detect samples with extreme outlier values ( $> 3$  standard deviations from any expected cluster). A European cluster was defined by including only individuals falling within a defined cluster with GBR individuals and self-reporting as White ethnicity. Quality controlled SNPs and individuals were taken forwards for genotype imputation which was undertaken on the Michigan Imputation server using the TopMed reference panel using recommended settings<sup>45</sup>. Files were converted to MACH format using DosageConverter (version 1.0.4, <https://genome.sph.umich.edu/wiki/DosageConverter>).

HLA imputation was performed using the Multi-Ethnic HLA reference panel (version 1.0 2021) available on the Michigan imputation server<sup>46</sup> using recommended settings. Phasing of multi-allelic

HLA alleles was undertaken using PHASE (version 2.1.1)<sup>47</sup>. HLA typing was also performed using PCR-sequence specific primers (SSP) at the Histogenetic laboratory, Oxford University NHS Foundation Trust, Oxford, UK.

#### **Structural analyses.**

The ternary HLA-DQA1\*01:02–HLA-DQB1\*06:02–Spike peptide complex was modelled using AlphaFold<sup>30</sup> available on Google Colaboratory server<sup>48</sup>. Structures were analysed and displayed using the PyMOL Molecular Graphics System, version 2.3.2. from Schrödinger, LLC

#### **Follow up functional assays.**

Samples at baseline (D0) and 28 days post-boost (D84) from 20 healthy adult volunteers participating in COV001 and COV002 who had received a two dose ChAdOx1 nCoV-19 vaccine schedule of either two standard doses, or one standard dose and one low dose were chosen for further functional work. Samples were evenly stratified by dose of second vaccine across individuals who either carried HLA-DQB1\*06 (with no HLA-DQB1\*05) and HLA-DQB1\*05 carriers (not carrying HLA-DQB1\*06).

For the proliferation assay, cryopreserved PBMC were washed twice with sterile DPBS and incubated with CellTrace Violet (Life Technologies), a free amine binding dye, at a final concentration of 2.5  $\mu$ M in PBS for 10 minutes at RT, protected from light. To quench any dye remaining in solution, cells were incubated with FBS for 5 minutes at 4°C. Cells were then resuspended in RPMI-1640 media supplemented with 1% L-glutamine, 1% penicillin streptomycin and 10% human AB serum (Sigma) and 250,000 cells were seeded per condition in U bottom 96-well tissue culture plates. Cells were stimulated with 15-mer peptides overlapping by 10 amino acids, comprising the length of the S1 or the S2 domain of the SARS-CoV-2 spike protein (ProImmune) at a final concentration of 1  $\mu$ g/ml. 2  $\mu$ g/ml of PHA served as a positive control and cells incubated with 0.13% DMSO (Sigma) in cell media was used as a negative control. Cells were then incubated for 7 days at 37°C, with 5% CO<sub>2</sub> and 95%

humidity and the media was changed on day 4. At the end of the incubation period, cells were stained with anti-human CD3-FITC (OKT3, Invitrogen), CD4-APC (RPA-T4, Invitrogen), CD8-PE-Cyanine7 (OKT8, Invitrogen), and Live/Dead near Infra-red stain (Invitrogen) prior to acquisition on a five-laser LSRFortessa X-20 flow cytometer (BD Biosciences) using FACSDiva v8.02 (BD Biosciences), and data were analysed in FlowJo v10.7. A hierarchical gating structure was applied, and data is presented as background subtracted.

For the T-cell activation induced marker assay, cryopreserved PBMCs from the same individuals were stimulated overnight (18 hours, 37°C, 5% CO<sub>2</sub>) at 2x10<sup>6</sup> cells per tube in rounded 5ml polystyrene U-bottom tubes (Falcon). Samples were stimulated with anti-CD28 (CD28.2, 1µg/ml, Invitrogen) and anti-CD49d (9F10, 1µg/ml, Invitrogen) alongside either a SARS-CoV-2 S1/S2 peptide megapool (134 peptides, 2µg/ml per peptide, ProImmune) or anti-CD3 (OKT3, Tonbo Biosciences) as a positive control.

Samples were stained with αCCR7-PE-Cy7 (G043H7, Biolegend) for 10 minutes at 37°C prior to the addition of the following antibodies and incubated for 30mins at room temperature: αCD3-BV711 (UCHT1, BD Biosciences), αCD4-PerCP-Cy5.5 (RPA-T4, Biolegend), αCD8-BV650 (RPA-T8, Biolegend), αCD14-APC-Cy7 (HCD14, Biolegend), αCD19-APC-Cy7 (HIB19, Biolegend), LIVE/DEAD Fixable Near IR (Invitrogen), αCD137-PE-Cy5 (4B4-1, Biolegend), αOX40-APC (Ber-ACT, Biolegend), αCD69-BUV395(FN50, BD Biosciences), αCCR6-PE (G034E3, Biolegend), αCXCR5-PE Dazzle 594 (J252D4, Biolegend), PD1-BV510 (EH 12.1, BD Biosciences), CXCR3-FITC (G025H7, Biolegend), CD45RA-AF700 (H1100, Biolegend), CCR7-PE-Cy7 (G043H7, Biolegend). Samples were acquired using a BD LSRFortessa Cell Analyzer.

Memory B cells were differentiated into antibody-secreting plasma cells for the detection of IgG responses using Enzyme-linked immunospot (ELISpot) according to the following steps.

Cryopreserved PBMCs from the same individuals were isolated from heparinized whole blood and resuspended at a final concentration of 2x10<sup>6</sup> cells/ml in Complete Medium (CM). CM was prepared



by combining RPMI (450ml, R-5886, Merck-Sigma), FBS-HI (50ml, F9665, Merck-Sigma), penicillin/streptomycin (5ml, P-4458, Merck-Sigma), L-Glutamine (5ml, G-7513, Merck-Sigma), NEAA (5ml, 11140035, Life Technologies), Sodium Pyruvate (5ml, 11360039, Life Technologies), and 2-Mercaptoethanol (5002µl, 31350010, Life Technologies). 10ml of polyclonal stimulants antigen mix (CpG (tlrl-2006-5, InvivGen SAS)+ SAC (507861-50, VWR International Ltd)+ PWM (L-9370, Sigma)) was distributed in 1x96 well plate (650180, Greiner) at 100 µl/well. 100 µl/well of cell suspension was added to each well (giving  $2 \times 10^5$  cells/well) and incubated at 37°C/ 5% CO<sub>2</sub>/ 95% humidity for 5-6 days. Memory B cells were harvested from the 96-well plate by gentle re-suspension into a 30ml universal container (201150, Greiner), and washed 3 times. The final pellet was re-suspended in 1ml wash buffer for cell counting and resuspended in CM at  $2 \times 10^6$  cells/ml. ELISpot was performed as previously described<sup>49,50</sup>.

## Statistical analyses

### Discovery cohort

Antibody responses were log-transformed and density distribution plots inspected for overlap in density distributions between laboratories (MSD or PPD) and paired correlation between assays using results available from both laboratories performed on samples from the same individual. If the paired correlation was less than 0.7 or the density distributions did not overlap, traits were tested for association within assay type then meta-analysed, but if the paired correlation was greater than 0.7 and the density distributions overlapped, traits were quintile normalised (using the qqnorm() function in R) within assay platform groups and tested in a pooled analysis including assay type as a fixed effect covariate. Samples taken at Day 28 post-first dose were used for the primary analysis.

A linear mixed model was used to maximise power and account for the diverse population structure and potential unrecognised close (cryptic) relatedness between study participants. Age, sex, antibody assay platform and nucleocapsid positivity were included as fixed effect covariates for each association. Genotype and HLA-wide association analyses were performed using the 'mlma' function

819 in GCTA (version 1.24.4)<sup>51</sup> after generating a genetic relatedness matrix (GRM) using non-pruned  
820 genotyped SNPs. The GRM was modelled as a random effect covariate with age (in years), sex,  
821 antibody assay laboratory and likelihood of natural exposure (based on anti-nucleocapsid protein  
822 antibodies (anti-N) >1000) coded as a binary variable included as fixed effect covariates for the  
823 primary genome-wide association study.

824 Sensitivity analyses for the genetic components included a further round of association analyses  
825 incorporating the first ten principal components for all individuals calculated within-cohort, and a  
826 further round of normalisation on the within-assay normalised RBD distributions.

827 Comparisons between imputed and classically typed HLA alleles were undertaken at the 4-digit (i.e.  
828 2-field) level of resolution. If a classically typed available call at a single allele locus included several  
829 potential higher resolution alleles (i.e. a list of potential ambiguities) only the first available allele call  
830 (adhering to a CWD priority) was used for comparison. If types were available to 6- or 8- digit  
831 resolution, the calls were reduced to 4-digit resolution for comparison between call types. The  
832 classical types were treated as the 'truth' set. By comparing each individual allele in turn it was  
833 possible to define calls of the imputed (or 'test') set that were:

- 834 • True positives (TP)
- 835 • False positives (FP); called by the test as that allele when it was in fact another allele  
836 according to the truth)
- 837 • False negatives (FN; called by the test as another allele when it was in fact this allele  
838 according to the truth)
- 839 • True negatives (TN).

840 Thus at the level of an individual allele various metrics could be calculated. Sensitivity was defined  
841 as:

842 
$$TP / (TP + FN)$$

843 Specificity was defined as:

844  $TN / (TN + FP)$

845 Positive predictive value (PPV) was defined as:

846  $TP / (TP + FP)$

847 Negative predictive value (NPV) was defined as:

848  $TN / (TN + FN)$

849 Accuracy was defined as:

850  $(TP + TN) / (TP + FP + FN + TN)$

851 Concordance was calculated at the level of the locus. For every pair of chromosomes with data  
852 available in both truth and test sets the number of identical allele calls between platforms was  
853 calculated and divided by the total number of alleles, equivalent to the positive predictive value  
854 (PPV). Any individual with missing alleles on either or both chromosomes on either platform were  
855 excluded from these calculations.

856 Univariate *P*-values were calculated using the Wilcoxon-rank test for continuous variables and Chi-  
857 squared Test for nominal variables. Permutation of Wilcoxon rank test of associating HLA alleles with  
858 RBD response was performed using the 'perm' package in R<sup>52</sup>. Adjusted Cox proportional hazards  
859 regression analyses for the breakthrough analyses were performed using the 'survival'<sup>53</sup> package in R  
860 and plots generated using 'survminer' and 'ggplot2'. The breakthrough infection definition above for  
861 the discovery cohorts was used as the outcome in the proportional hazards model with individuals  
862 censored at either time of breakthrough, date of withdrawal or the 10 October 2021, whichever  
863 came first. The effect of carriage of HLA-DQB1\*06 was estimated after adjustment for age (in years  
864 measured at baseline), healthcare worker status (defining whether individuals were healthcare  
865 workers and whether they cared for one, or more than one patient with COVID-19 per week), BMI

(less than 30 kg/m<sup>2</sup>, or equal to or greater than 30 kg/m<sup>2</sup>), ancestry (using the first two principal components of genetic variation to capture genetic structure), chronic health condition (presence of none, or one or more chronic respiratory, cardiovascular or diabetic health conditions). Using analyses undertaken on understanding the correlates of protection of ChAdOx1 nCoV-19<sup>13</sup> we aimed to perform an identical modelling exercise and thus samples were reweighted based on the interval between first and second vaccines (no second dose, <6, 6-8, 9-11 and ≥12 weeks) and dose arm of trial (standard dose (SD) alone, SD/SD, low dose (LD)/SD, SD/LD) distributions of individuals within the entire genotyped set with antibody data available using inverse probability weighting calculated using the 'ipw' package in R<sup>54</sup>. All analyses were undertaken in R version 4.1.1, except estimation of the genomic inflation factor ( $\lambda$ ) which was undertaken in R version 3.6.2 using the GenABEL package<sup>55</sup>.

#### Replication cohort

Individuals from all three replication cohorts were stratified by HLA-DQB1\*06 and DRB1-71E/R status and tested for association with log<sub>10</sub>-transformed anti-S antibody levels measured following the first vaccine dose (and before the second vaccine) using linear regression adjusting for age, sex, self-reported ethnicity, priming vaccine, study and interval between prime and blood sample in days. Individuals were either analysed together or stratified according to first vaccine dose received (ChAdOx1 nCoV-19 or BNT162b2). Survival analyses were performed using the same methods as for the discovery cohorts but including only age, sex, and first vaccine type received as covariates with reweighting performed using interval between first and second vaccines in days. Censoring was undertaken at point of breakthrough infection, withdrawal from study or date of database locking (21 January 2022 for COMCOV/COMCOV2 or 29 November 2021 for COV006), whichever came soonest. Healthcare worker status, BMI and chronic health condition information was not available for COV006 and so the variables were not included in the final replication analysis. All replication analyses were performed in R version 4.1.1.

892 [Data availability](#)

893 The University of Oxford is committed to providing access to anonymized data for non-commercial  
894 research. Participants genotype and phenotype data will be deposited on European Genome  
895 Phenome Archive and will be made available for non-commercial use only (DUO:0000046).

896

897

898

899 Oxford COVID Vaccine Trial Genetics Study Team Group

900

901 Ana Cavey<sup>7</sup>, Angela Minassian<sup>2,8</sup>, Arabella Stuart<sup>2</sup>, Baktash Khozoe<sup>4</sup>, Brama Hanumunthadu<sup>2</sup>, Brian  
902 Angus<sup>4</sup>, Catherine C Smith<sup>2</sup>, Iain Turnbull<sup>9</sup>, Jonathan Kwok<sup>10</sup>, Katherine R W Emary<sup>2</sup>, Liliana  
903 Cifuentes<sup>11</sup>, Maheshi N Ramasamy<sup>2</sup>, Paola Cicconi<sup>4</sup>, Adam Finn<sup>12</sup>, Alastair C McGregor<sup>13</sup>, Andrea M  
904 Collins<sup>14</sup>, Andrew Smith<sup>15</sup>, Anna L Goodman<sup>16,17</sup>, Christopher A Green<sup>18</sup>, Christopher J A Duncan<sup>19,20,21</sup>,  
905 Christopher J A Williams<sup>22</sup>, Daniela M Ferreira<sup>2,14</sup>, David P J Turner<sup>23</sup>, Emma C Thomson<sup>24</sup>, Helen  
906 Hill<sup>14</sup>, Katrina Pollock<sup>25</sup>, Mark Toshner<sup>26</sup>, Patrick J Lillie<sup>27</sup>, Paul Heath<sup>28,29</sup>, Rajeka Lazarus<sup>30</sup>, Rebecca K  
907 Sutherland<sup>31</sup>, Ruth O Payne<sup>32</sup>, Saul N Faust<sup>33,34</sup>, Tom Darton<sup>32</sup>, Vincenzo Libri<sup>35</sup>, Rachel Anslow<sup>2</sup>,  
908 Samuel Provtsgaard-Morys<sup>2</sup>, Thomas Hart<sup>2</sup>, Amy Beveridge<sup>2</sup>, Syed Adlou<sup>2</sup>

909

910

911 <sup>7</sup>Nuffield Department of Clinical Neurosciences, University of Oxford, Oxford, UK

912 <sup>8</sup>Department of Biochemistry, University of Oxford, Oxford UK

913 <sup>9</sup>Nuffield Department of Population Health, University of Oxford, Oxford, UK

914 <sup>10</sup>Nuffield Department of Medicine, University of Oxford, Oxford, UK

915 <sup>11</sup>Kennedy Institute of Rheumatology, Nuffield Department of Orthopaedics, The University of  
916 Oxford, UK

917 <sup>12</sup>School of Population Health Sciences, University of Bristol and University Hospitals Bristol and  
918 Weston NHS Foundation Trust, UK

919 <sup>13</sup>London Northwest University Healthcare, Harrow, UK

920 <sup>14</sup>Department of Clinical Sciences, Liverpool School of Tropical Medicine, Liverpool, UK

921 <sup>15</sup>College of Medical, Veterinary & Life Sciences, Glasgow Dental Hospital & School, University of  
922 Glasgow, Glasgow, UK

923 <sup>16</sup>Guy's and St Thomas' NHS Foundation Trust, London, UK

924 <sup>17</sup>MRC Clinical Trials Unit at UCL, London

925 <sup>18</sup>NIHR/Wellcome Trust Clinical Research Facility, University Hospitals Birmingham NHS Foundation  
926 Trust, Birmingham, UK

927 <sup>19</sup>Department of Infection and Tropical Medicine, Newcastle upon Tyne Hospitals NHS Foundation  
928 Trust, Newcastle, UK

929 <sup>20</sup>NIHR Newcastle Clinical Research Facility, Newcastle upon Tyne Hospitals NHS Foundation Trust,  
930 Newcastle, UK

931 <sup>21</sup>Translational and Clinical Research Institute, Immunity and Inflammation Theme, Newcastle  
932 University, UK

933 <sup>22</sup>Public Health Wales, Cardiff, Wales and Aneurin Bevan University Health Board, Wales

934 <sup>23</sup>School of Life Sciences, University of Nottingham and Nottingham University Hospitals NHS Trust,  
935 Nottingham, UK

936 <sup>24</sup>MRC - University of Glasgow Centre for Virus Research & Department of Infectious Diseases,  
937 Queen Elizabeth University Hospital, Glasgow, UK

938 <sup>25</sup>NIHR Imperial Clinical Research Facility and NIHR Imperial Biomedical Research Centre, London, UK

939 <sup>26</sup>Heart Lung Research Institute, Department of Medicine, Cambridge

940 <sup>27</sup>Hull University Teaching Hospitals NHS Trust, UK

941 <sup>28</sup>St George's Vaccine Institute, St George's, University of London, London, UK

942 <sup>29</sup>Department of Infection, Sheffield Teaching Hospitals NHS Foundation Trust, Sheffield, UK

943 <sup>30</sup>Severn Pathology, North Bristol NHS Trust, Bristol, UK

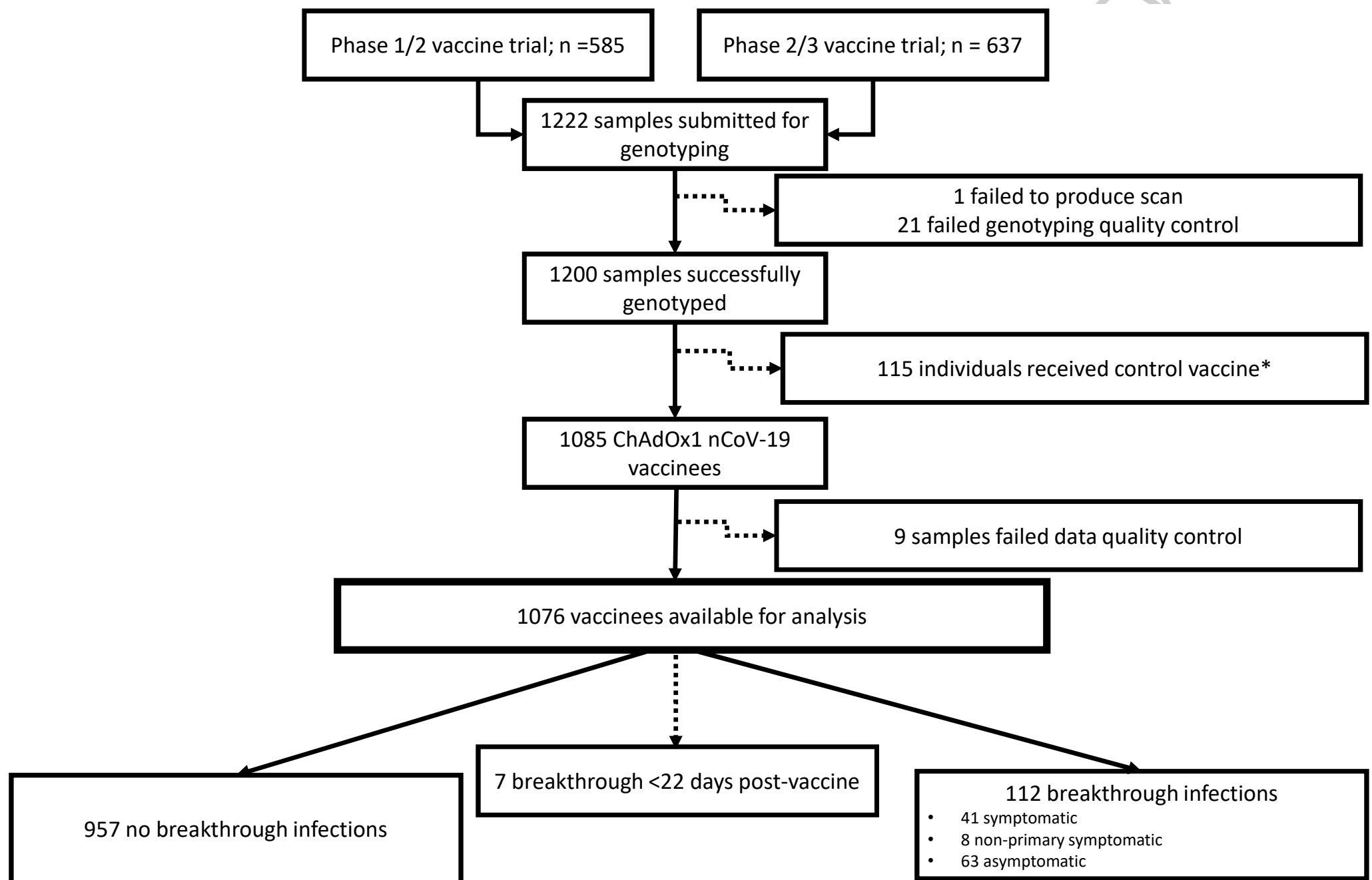
944 <sup>31</sup>Clinical Infection Research Group, Regional Infectious Diseases Unit, NHS Lothian, Edinburgh, UK

945 <sup>32</sup>Department of Infection, Immunity and Cardiovascular Diseases, University of Sheffield, Sheffield,  
946 UK

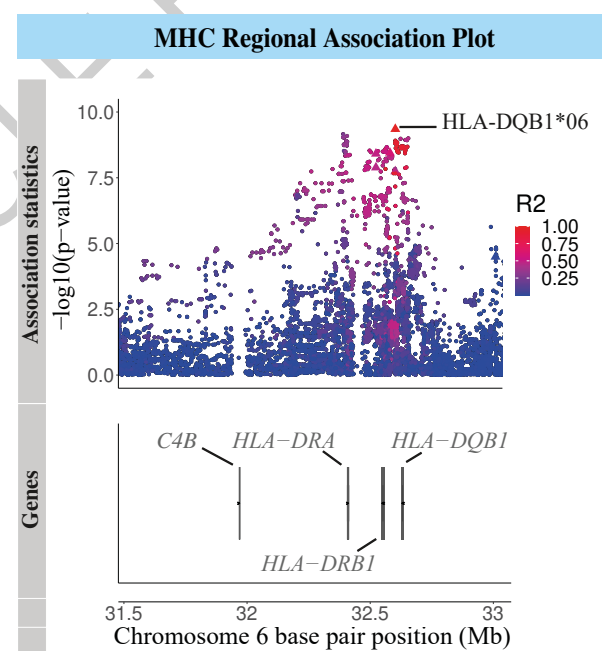
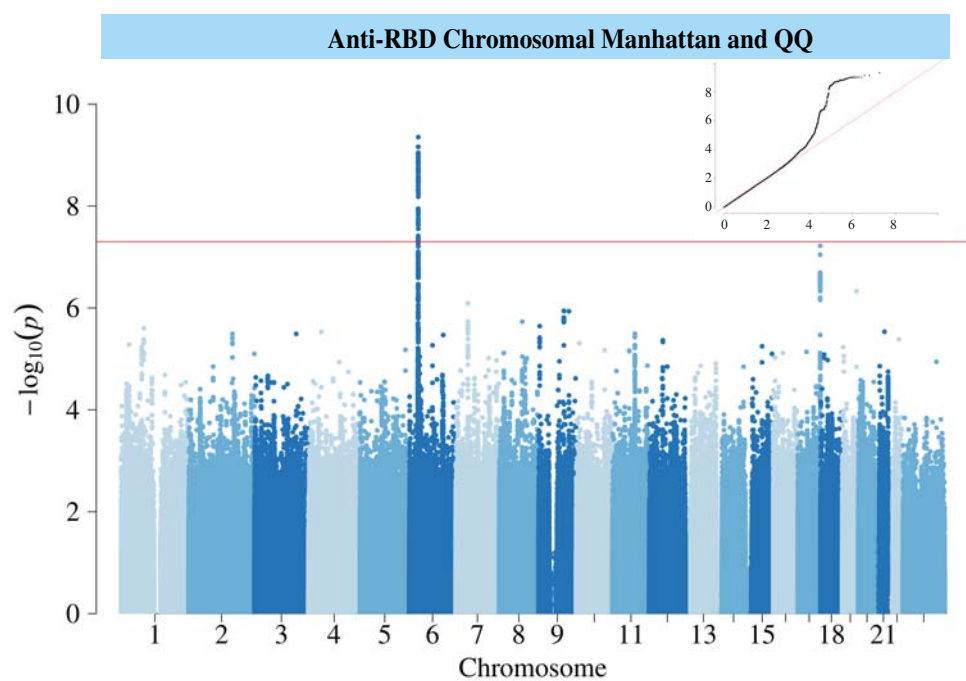
947 <sup>33</sup>NIHR Southampton Clinical Research Facility and Biomedical Research Centre, University Hospital  
948 Southampton NHS Foundation Trust, Southampton, UK

949 <sup>34</sup>Faculty of Medicine and Institute for Life Sciences, University of Southampton, Southampton, UK  
950 <sup>35</sup>NIHR UCLH Clinical Research Facility and NIHR UCLH Biomedical Research Centre, London, UK  
951

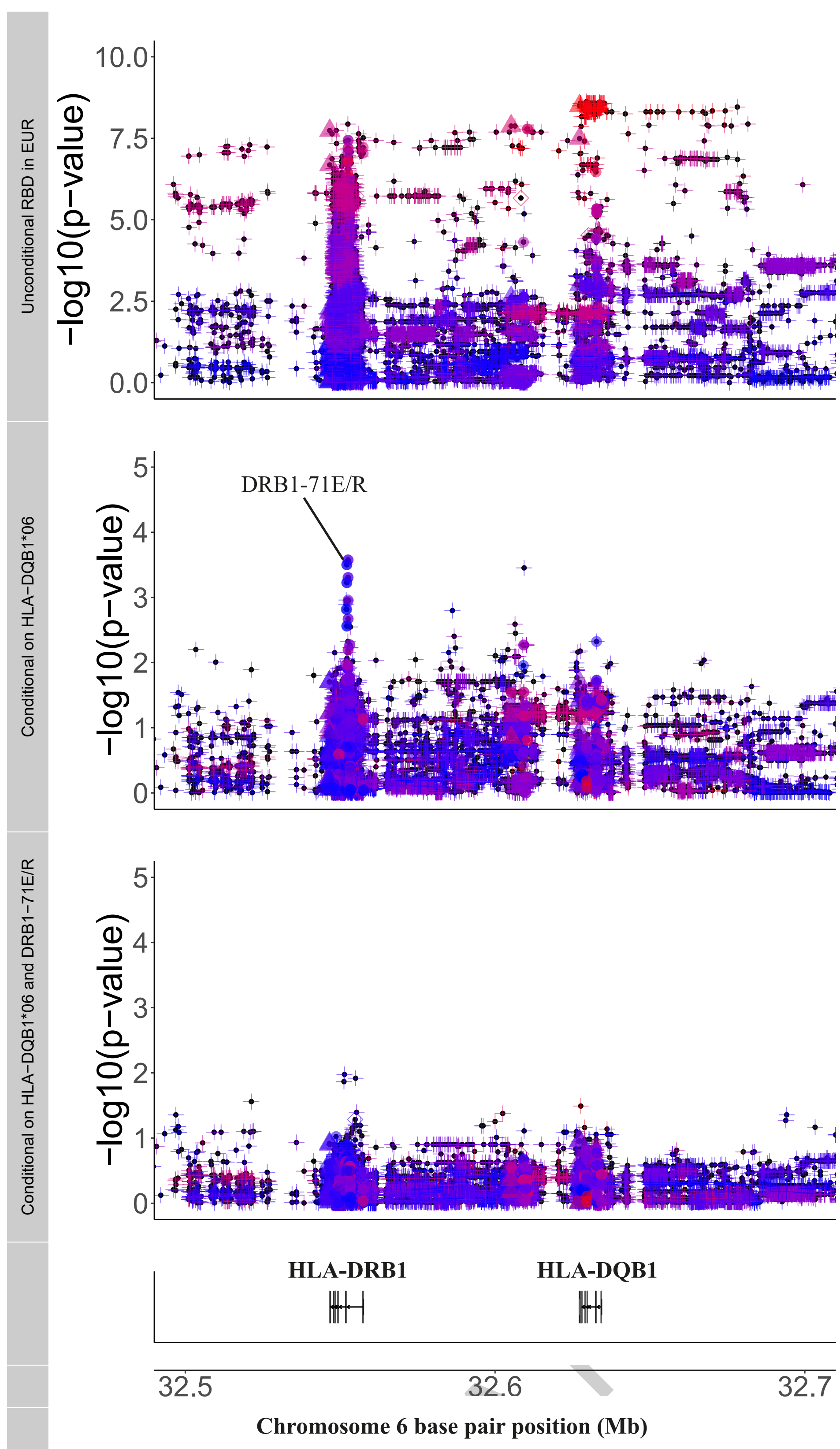
ACCELERATED ARTICLE PREVIEW



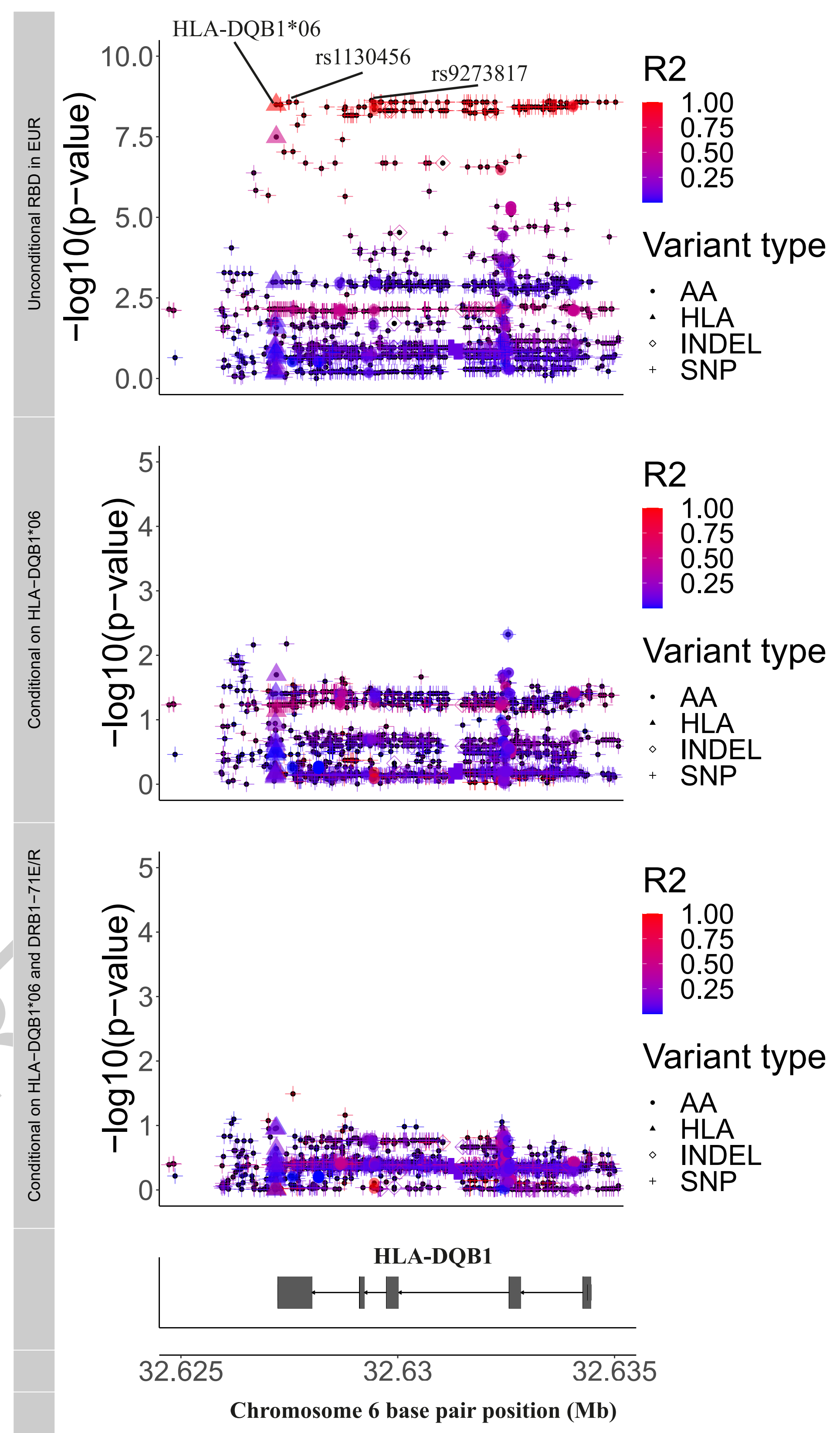




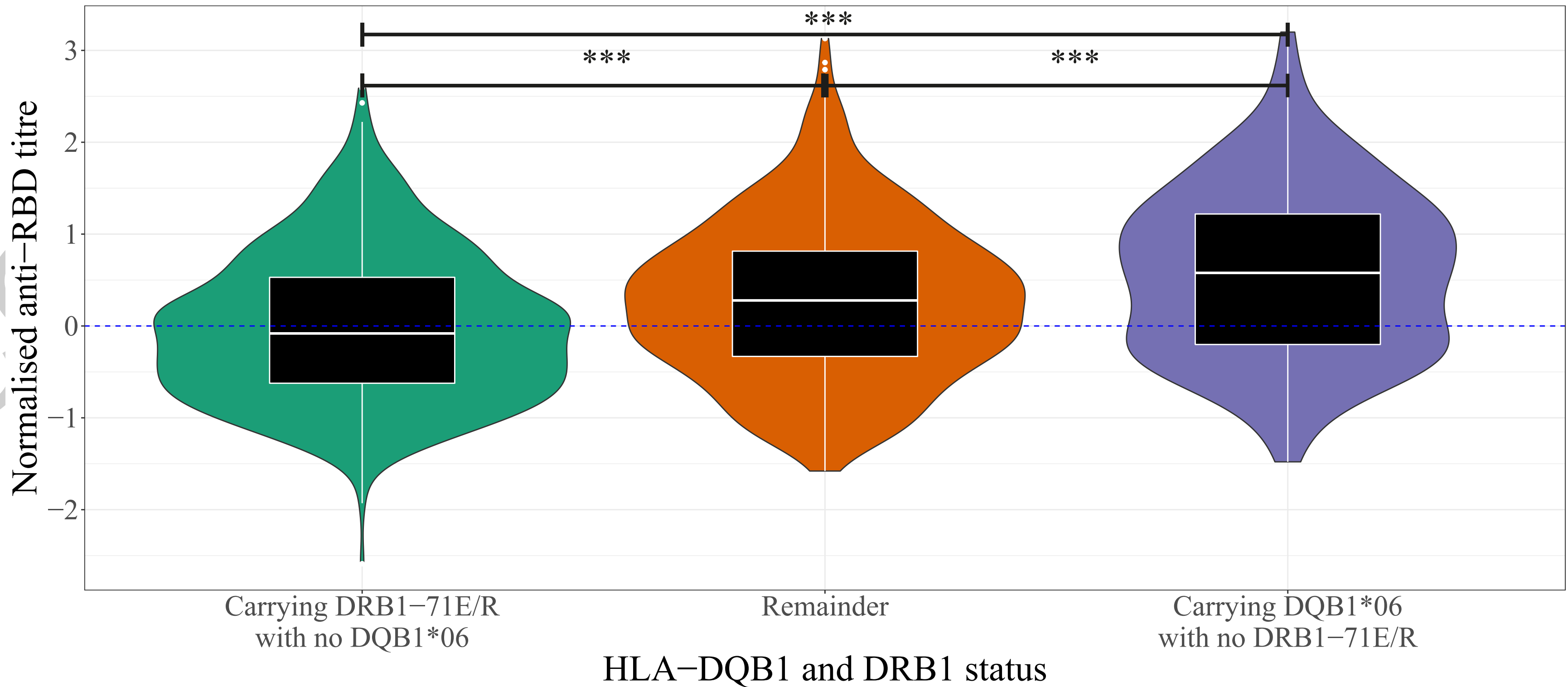
A



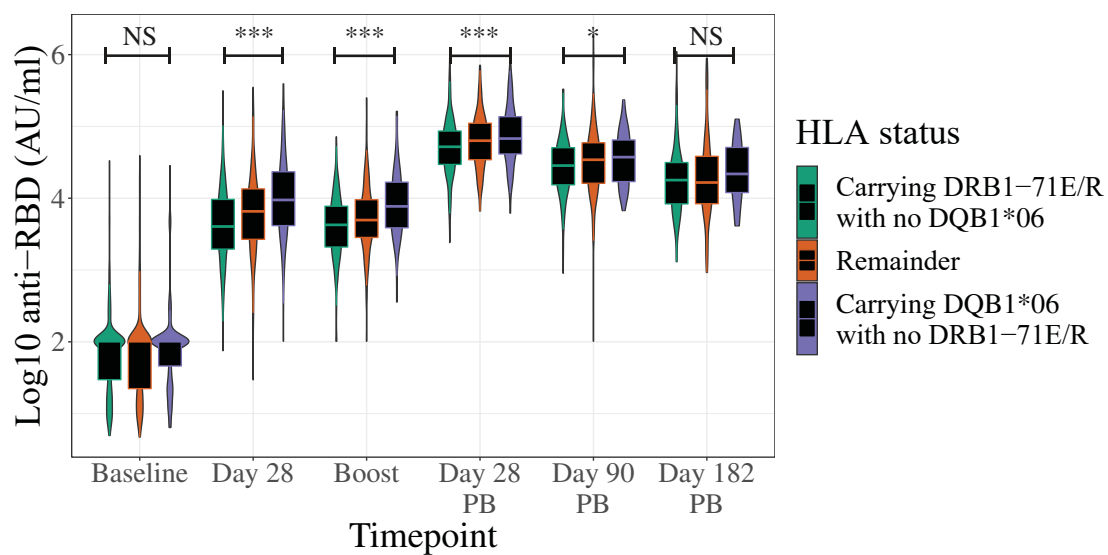
B



C

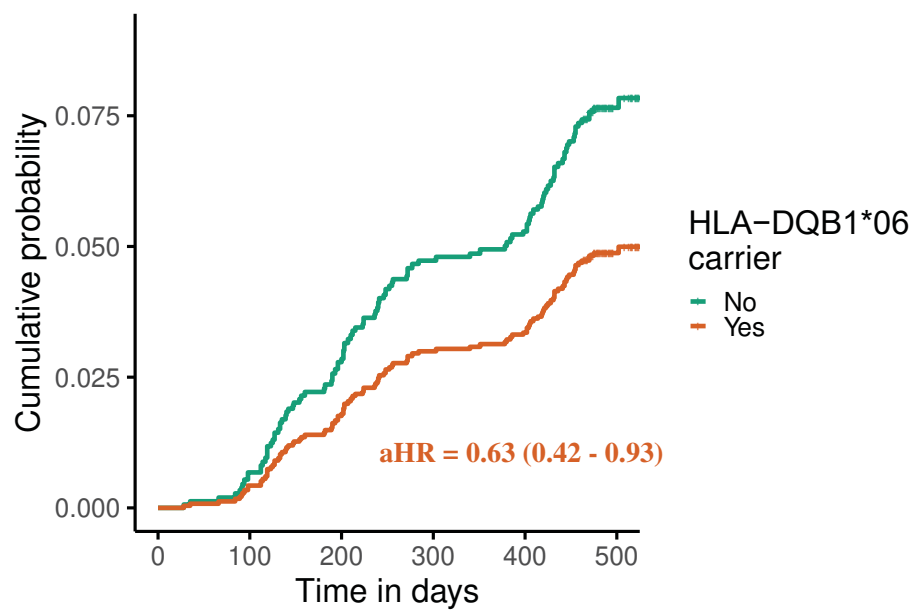


A

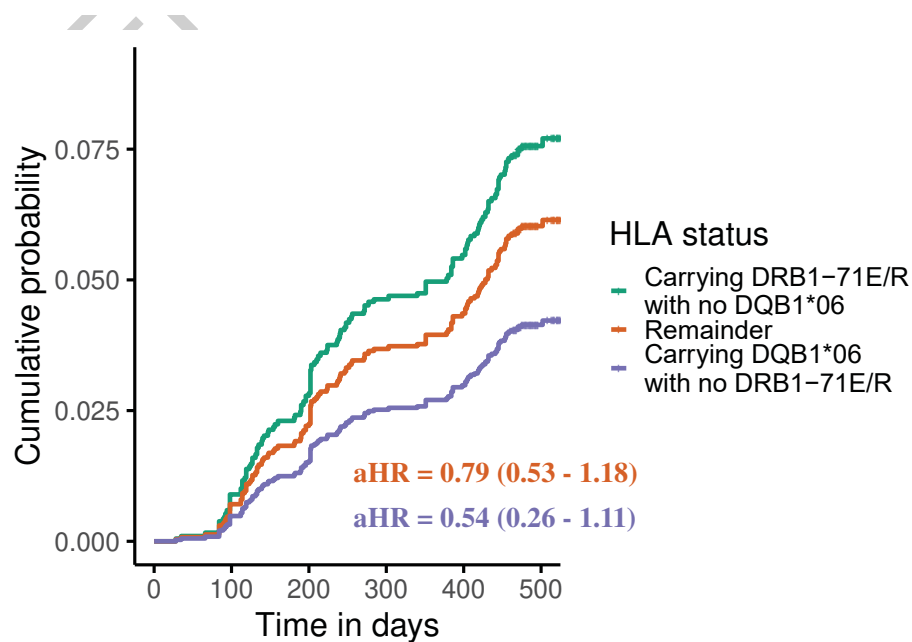


Carrying DRB1-71E/R with no DQB1*06	533	533	326	331	196	124
Carrying neither DQB1*05 or DQB1*06	419	419	251	353	163	108
Carrying DQB1*06 with no DQB1*05	125	125	81	82	54	32

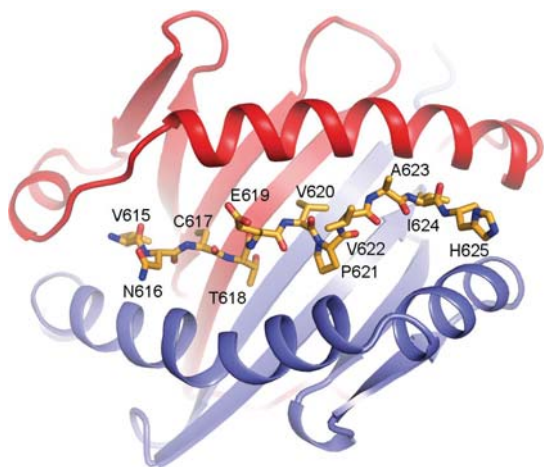
B



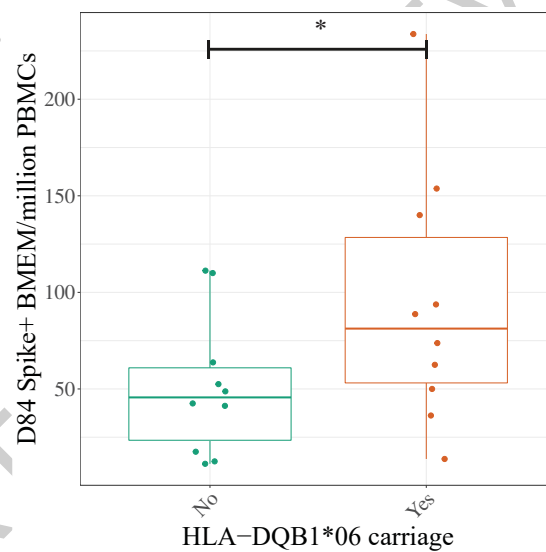
C



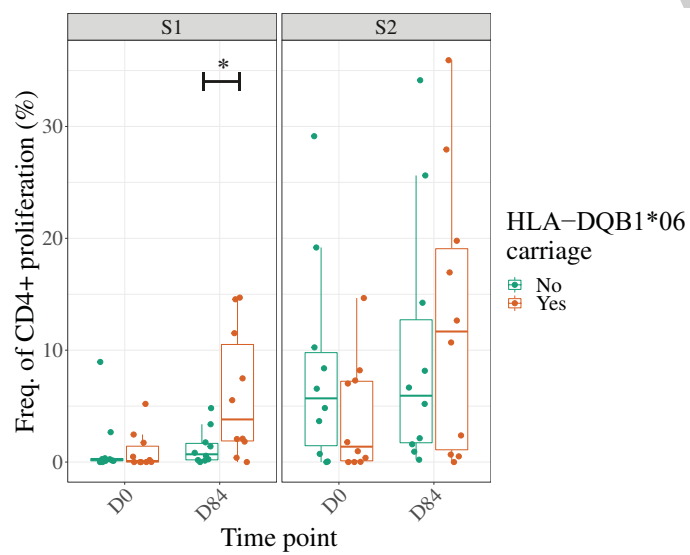
**A** DQA1\*01:02 - DQB1\*06:02 - Spike peptide (Alpha Fold)



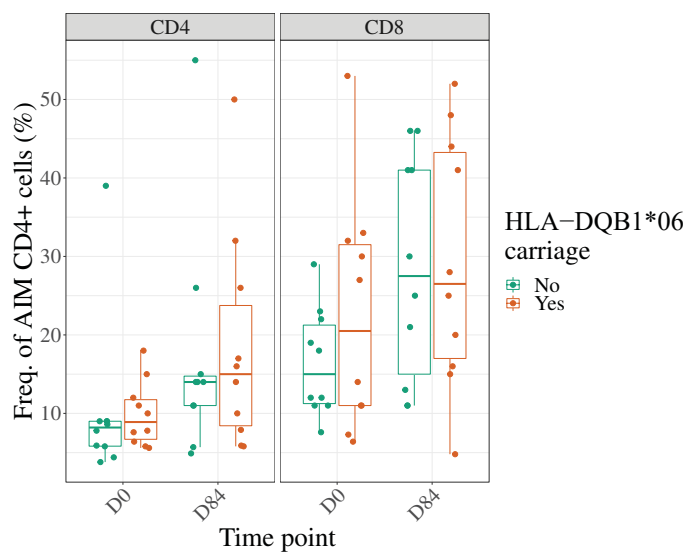
**B**



**C**



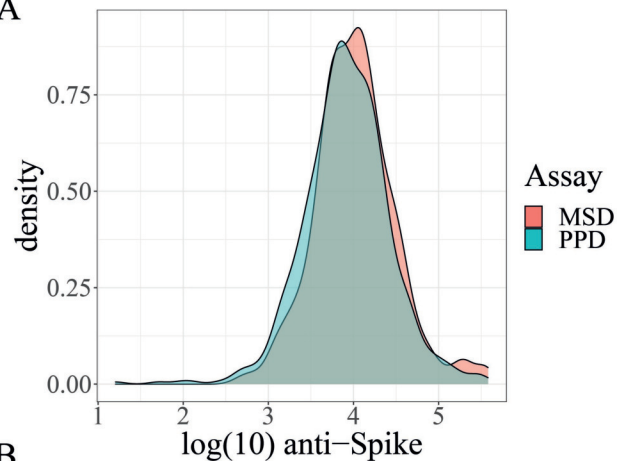
**D**



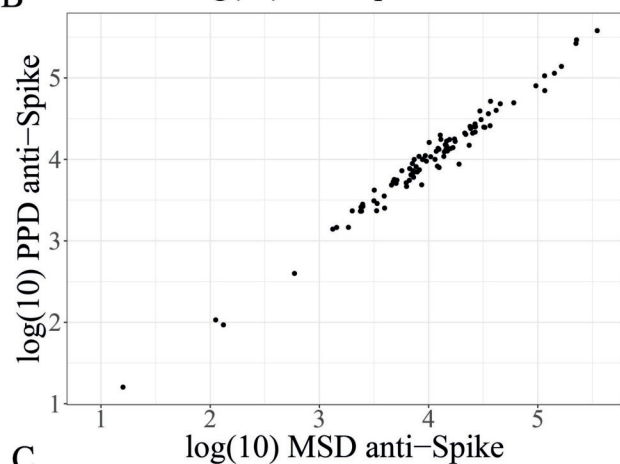


## Anti-Spike

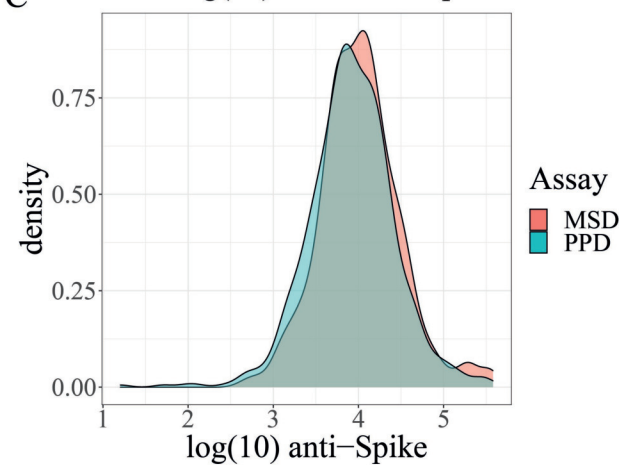
A



B

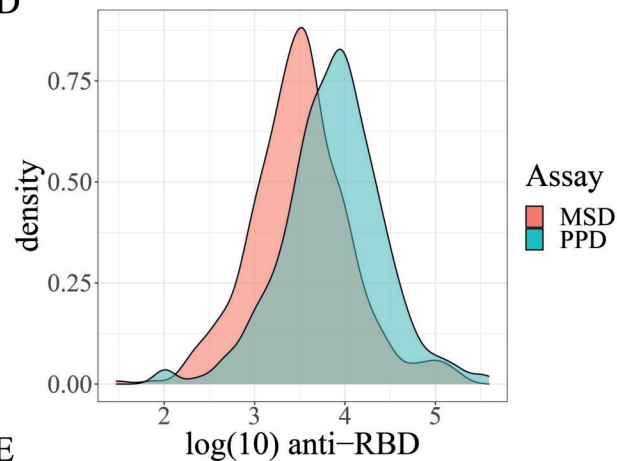


C

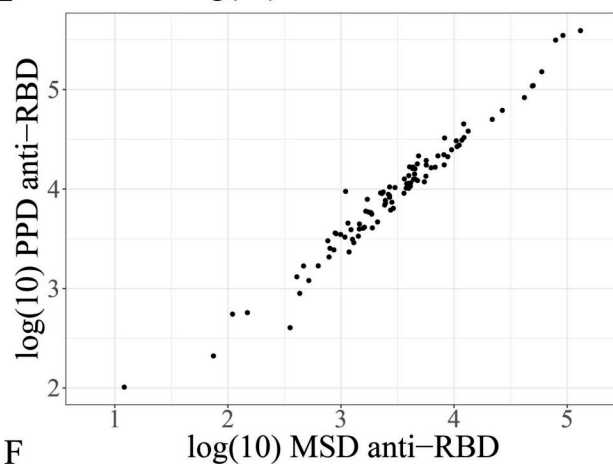


## Anti-Receptor Binding Domain

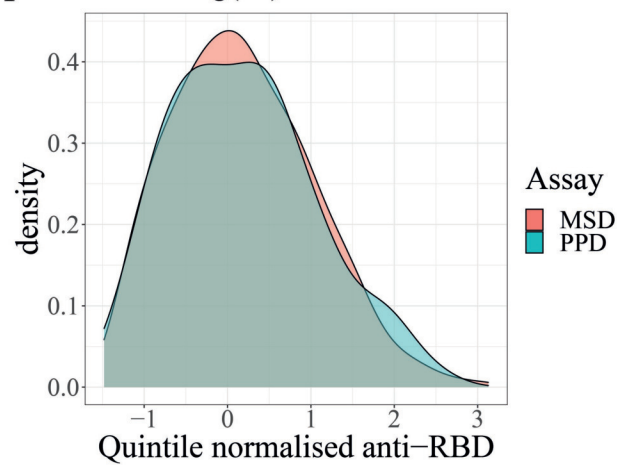
D



E

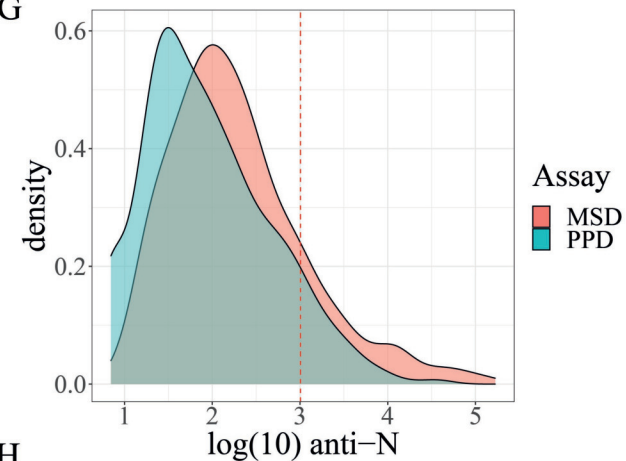


F

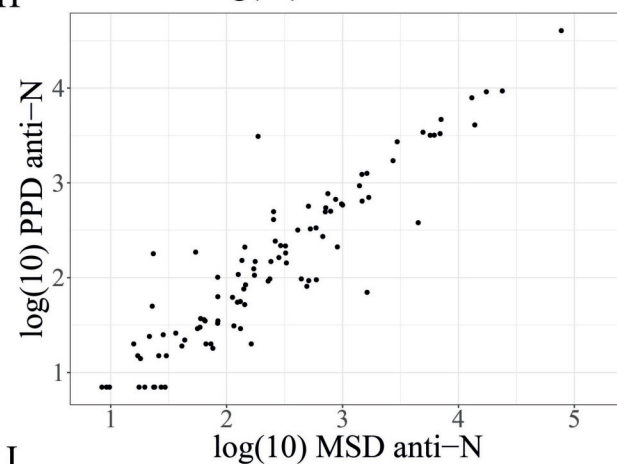


## Anti-Nucleocapsid

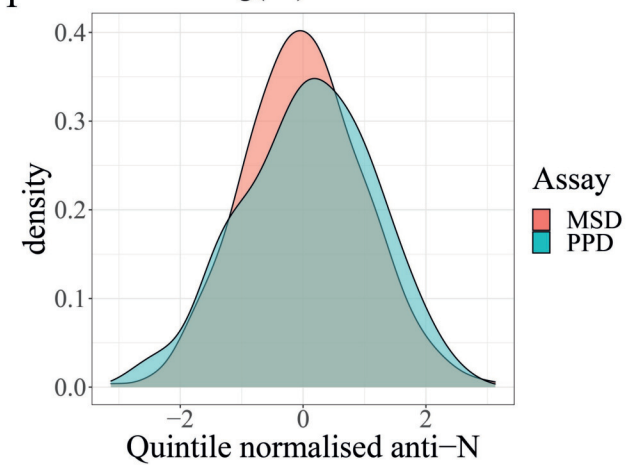
G

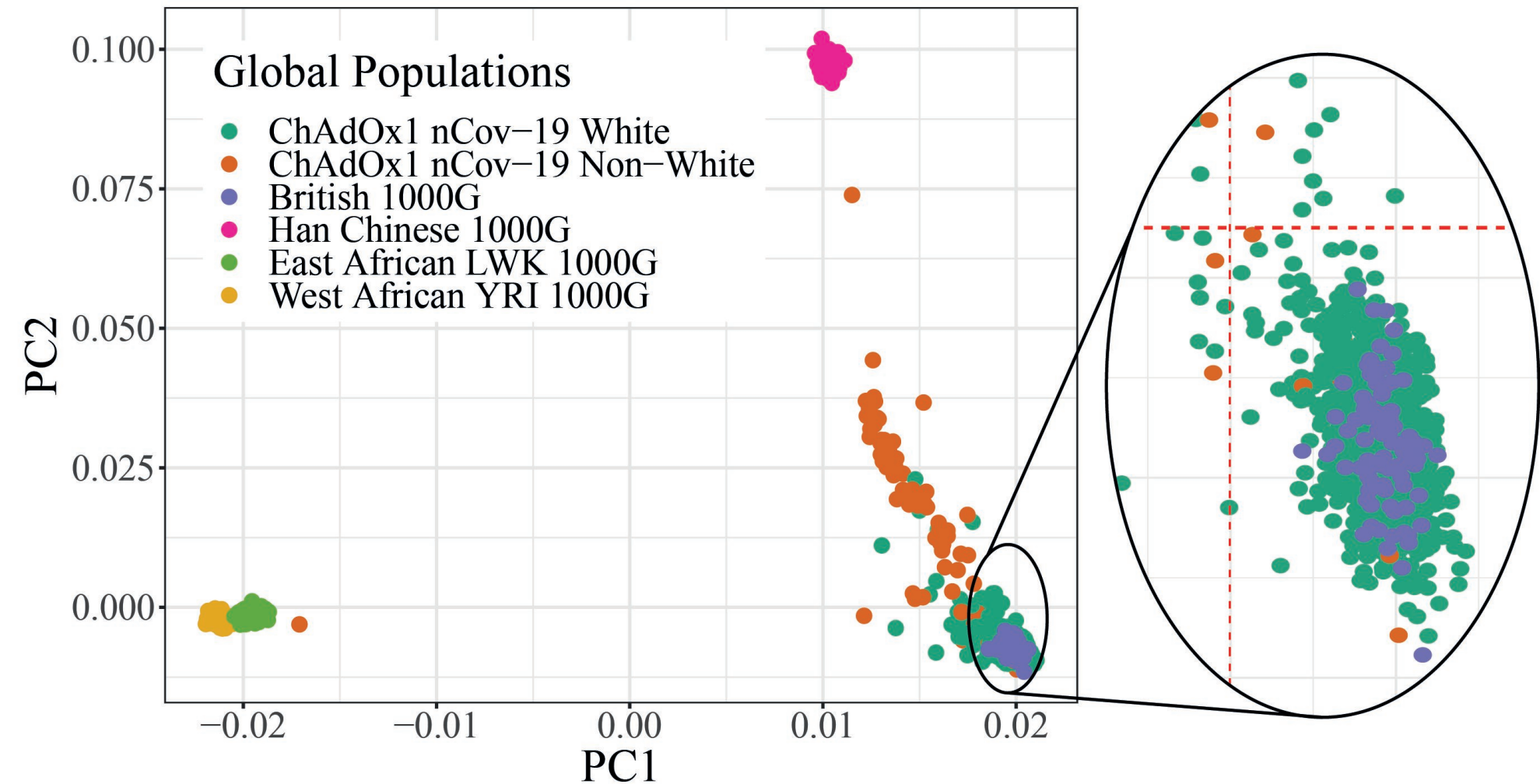


H

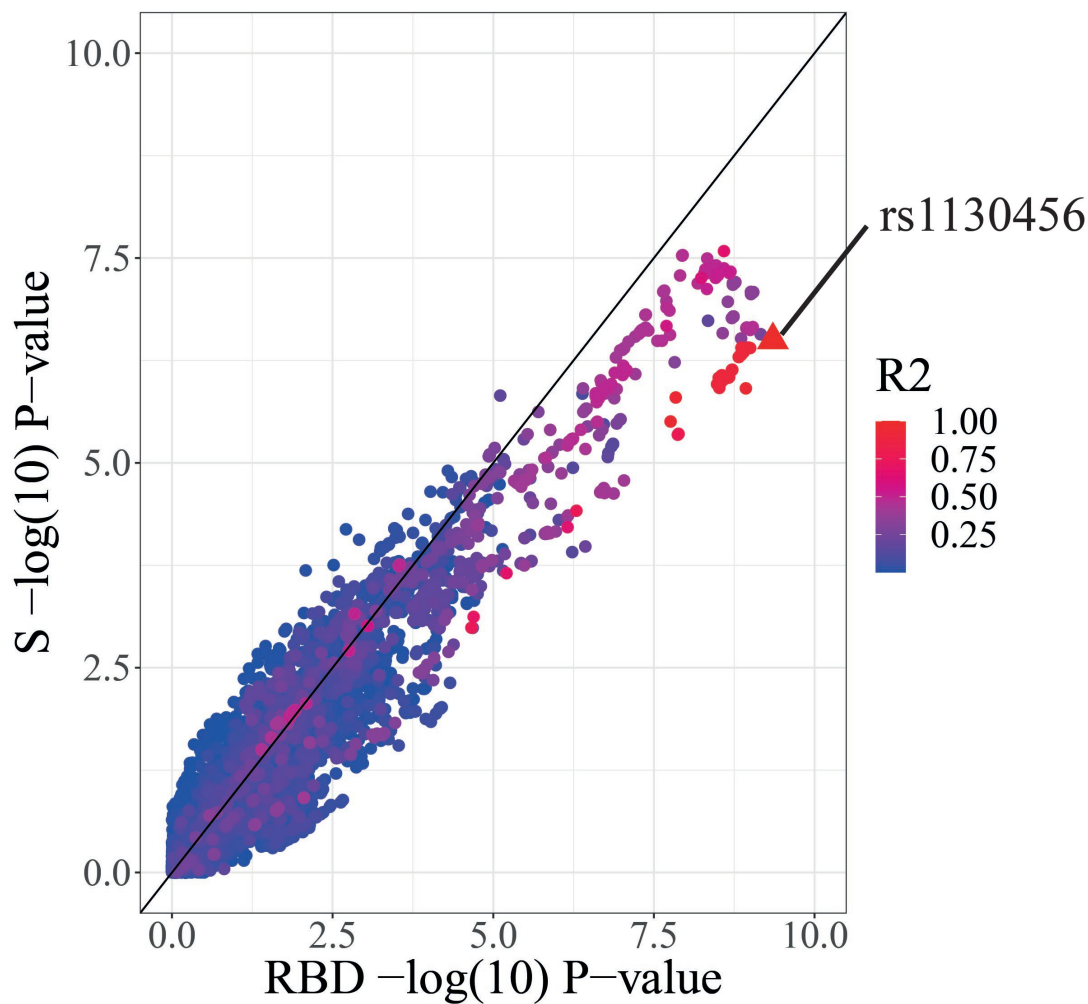


I

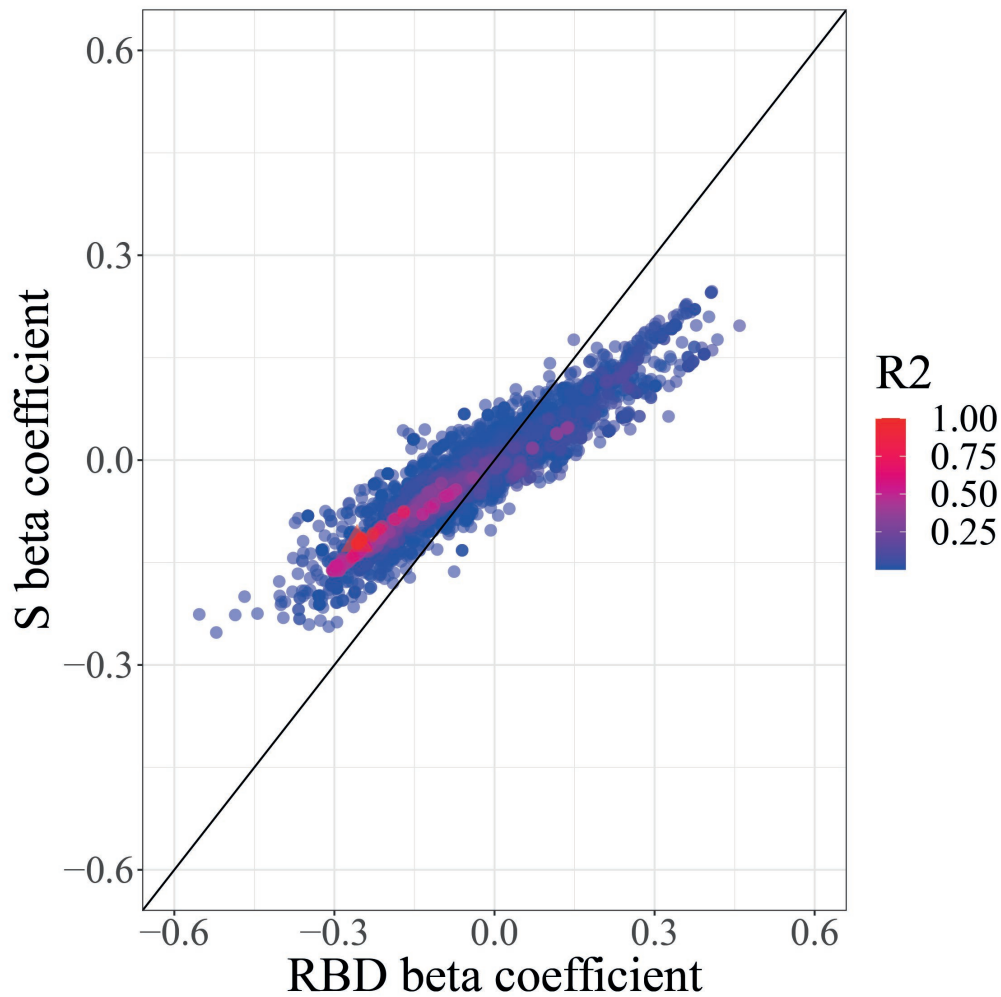


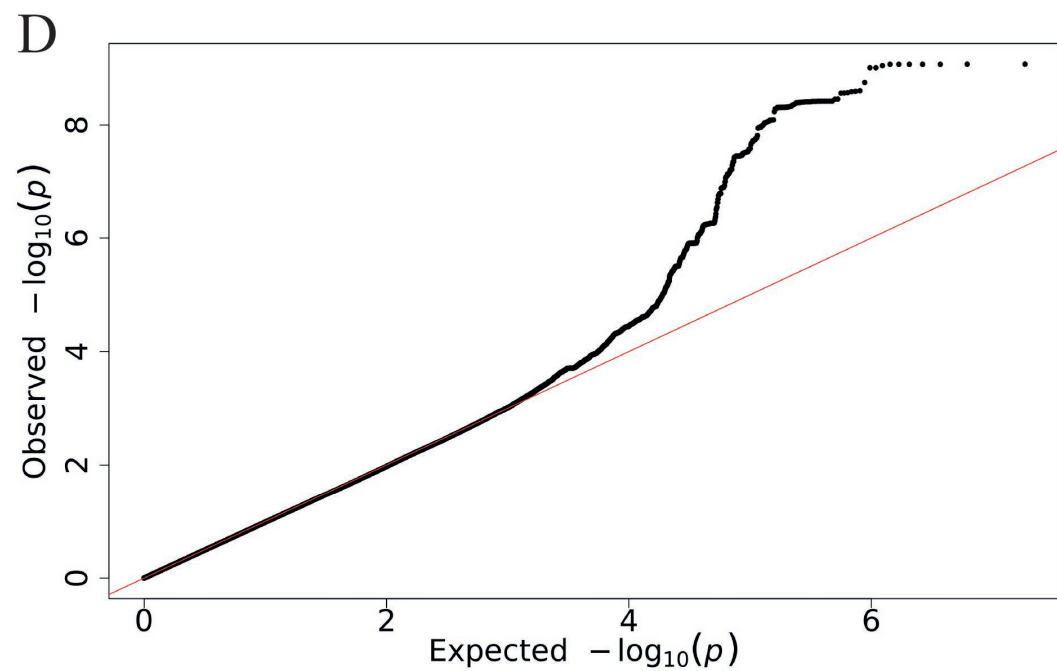
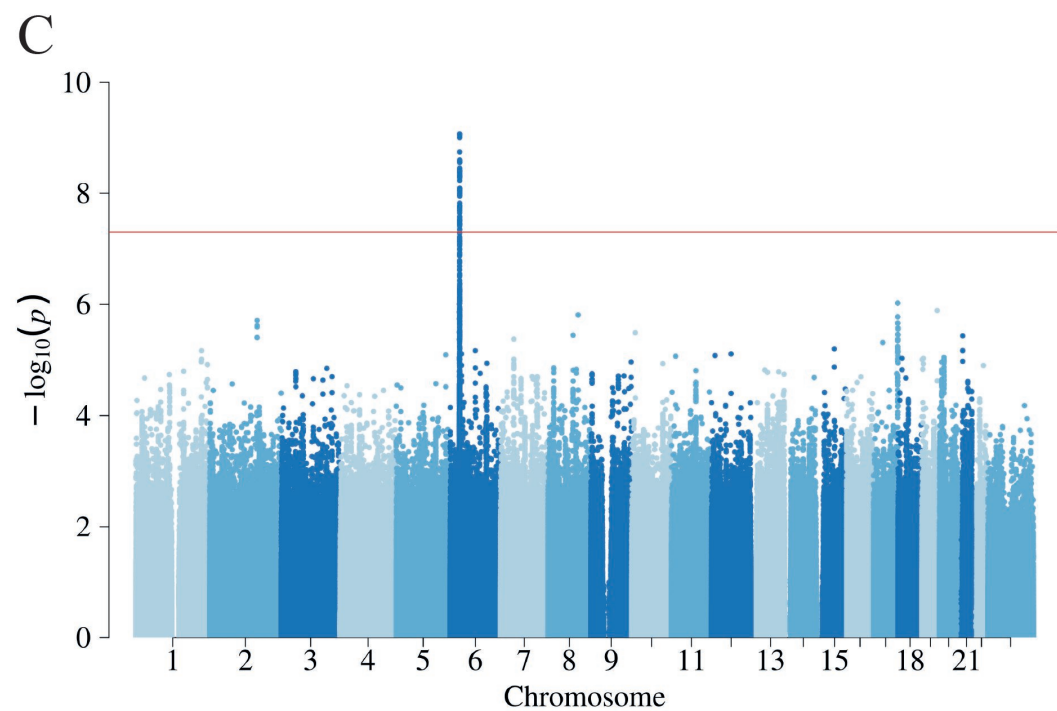
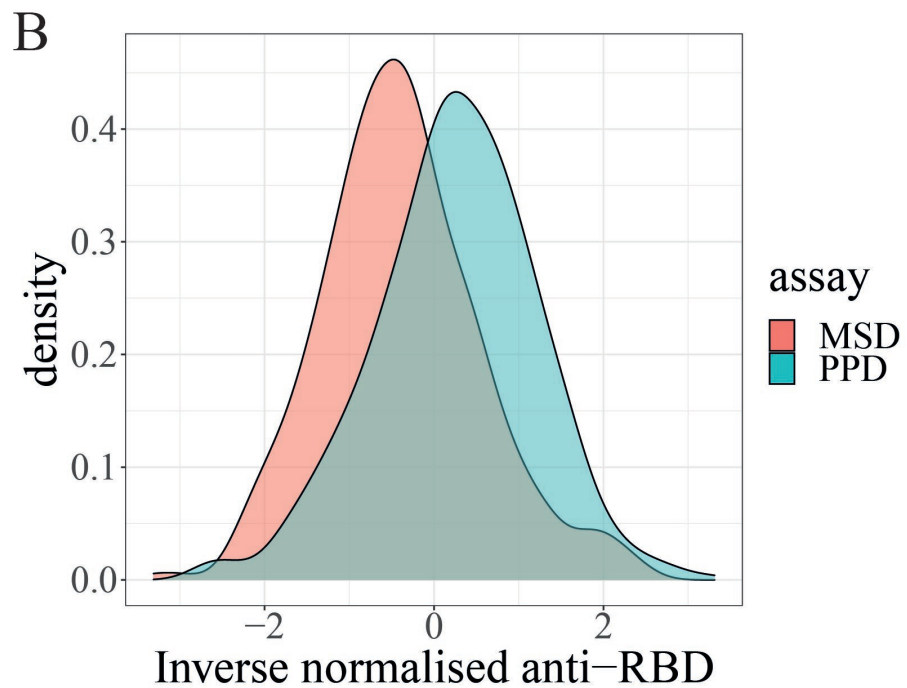
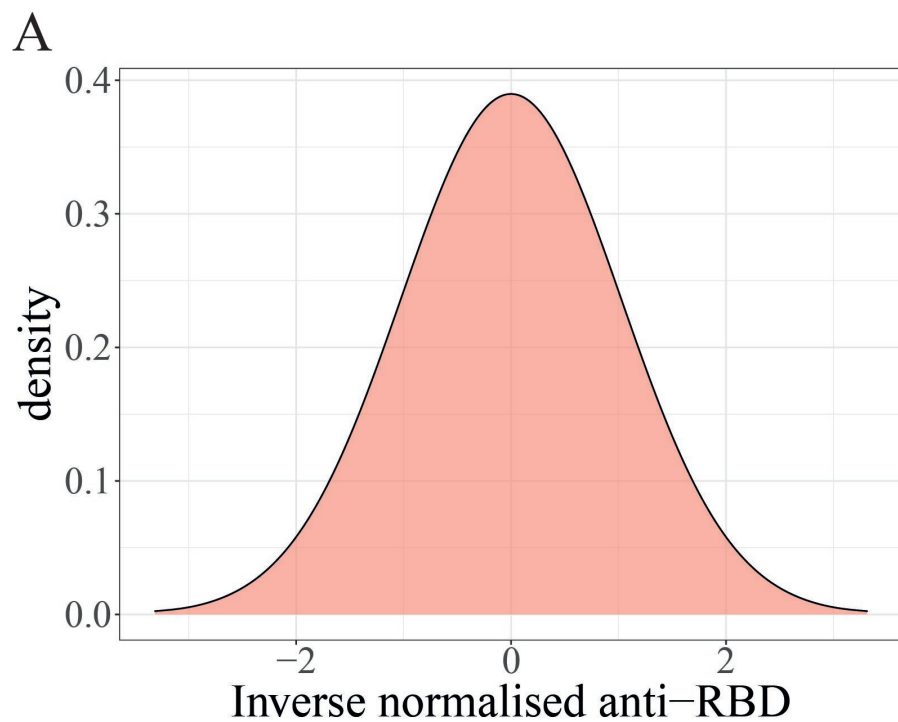


A



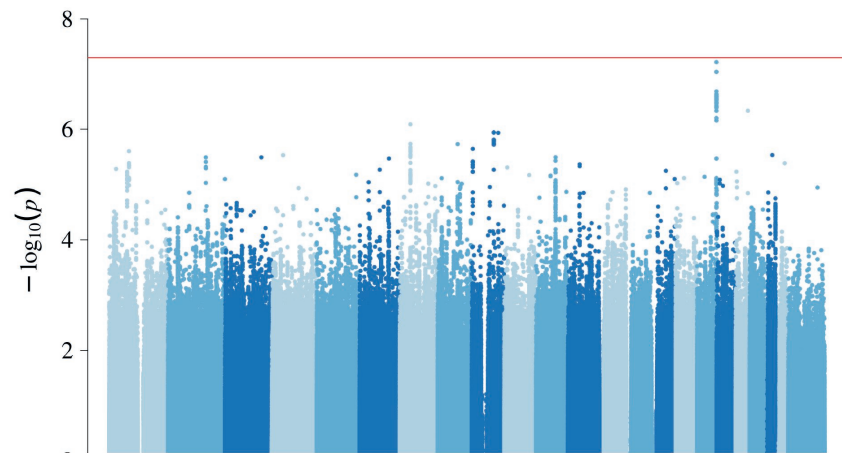
B



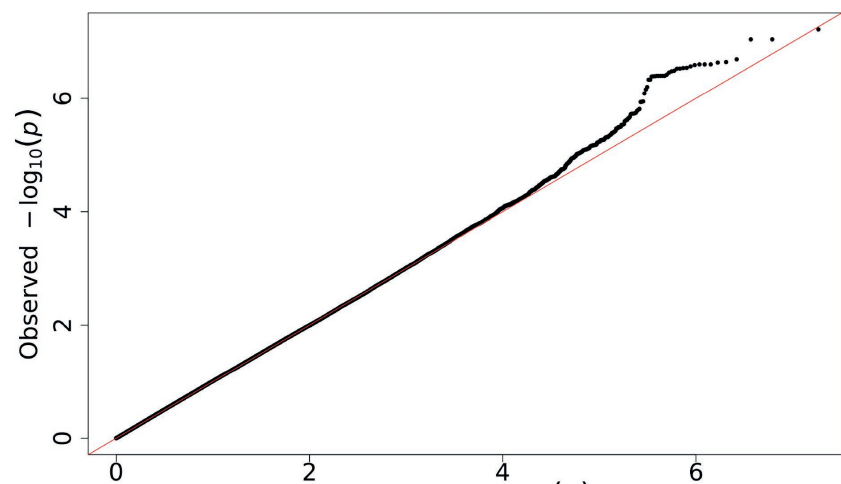




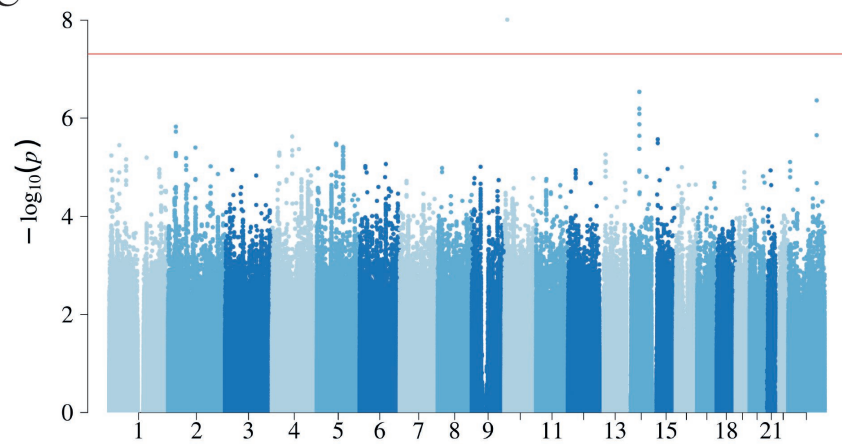
A



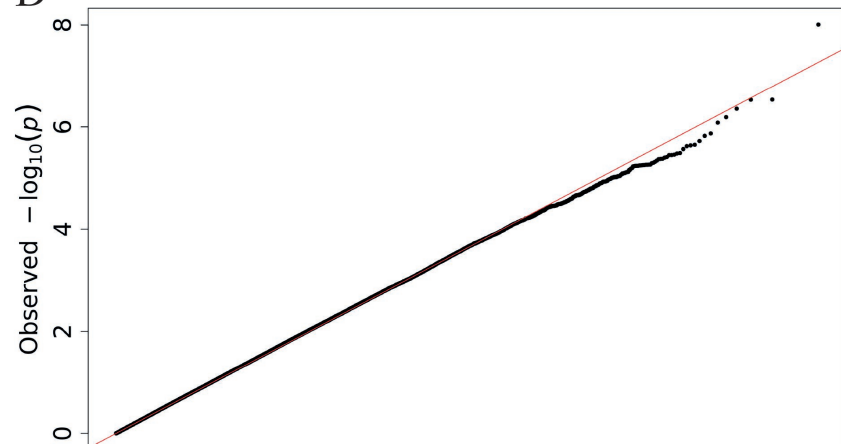
B



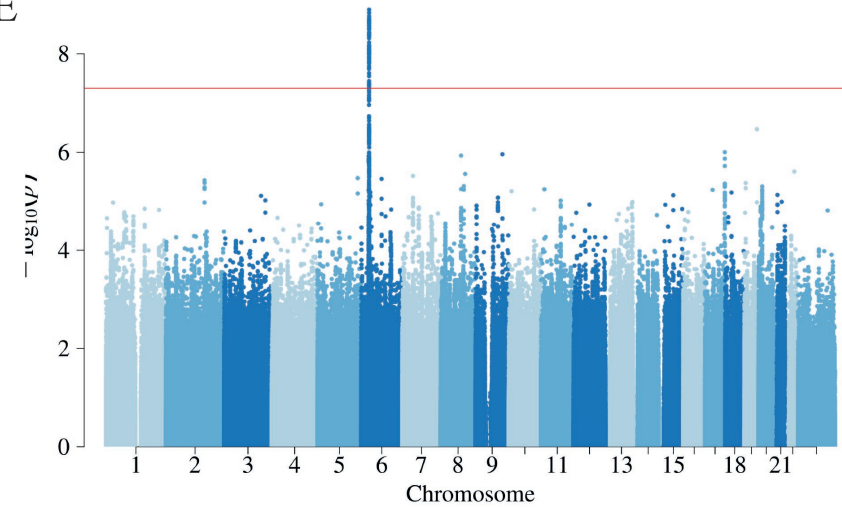
C



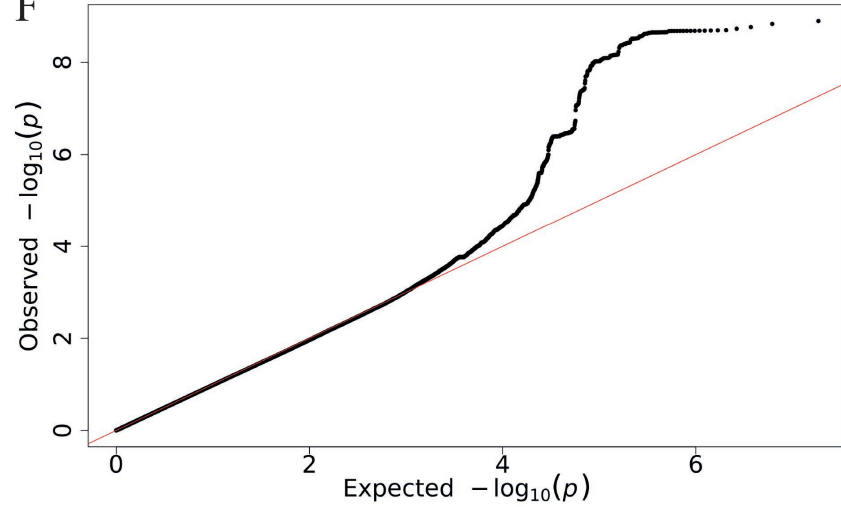
D

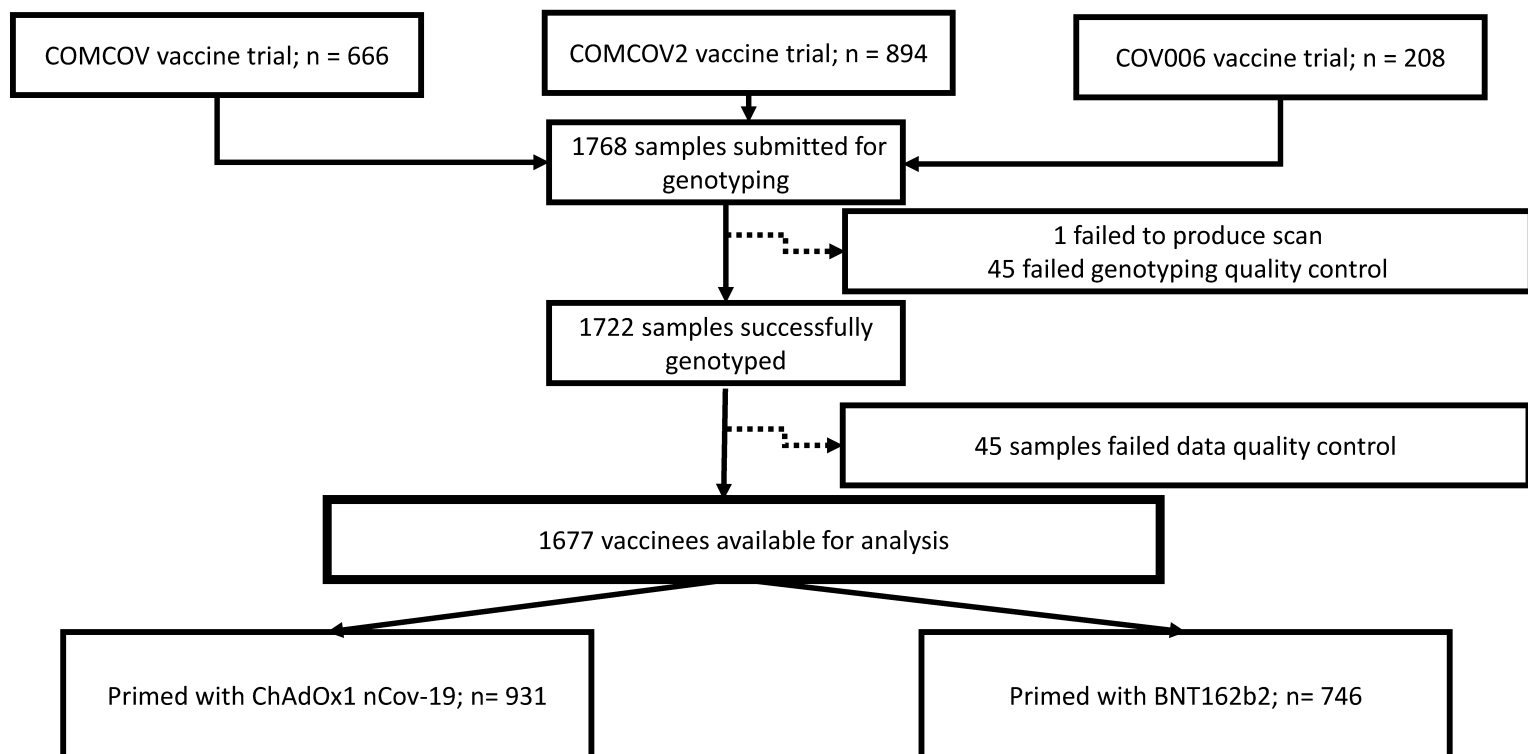


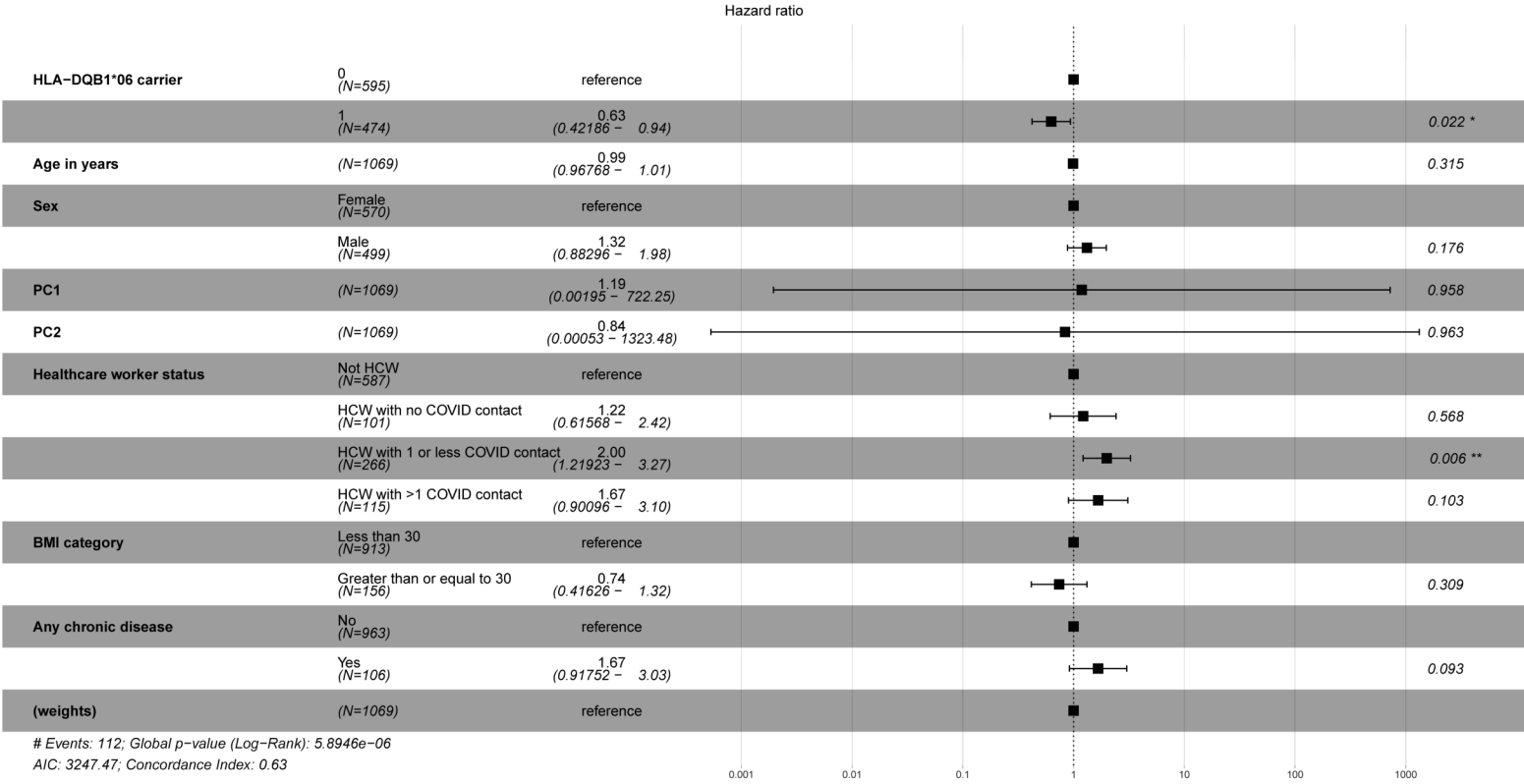
E

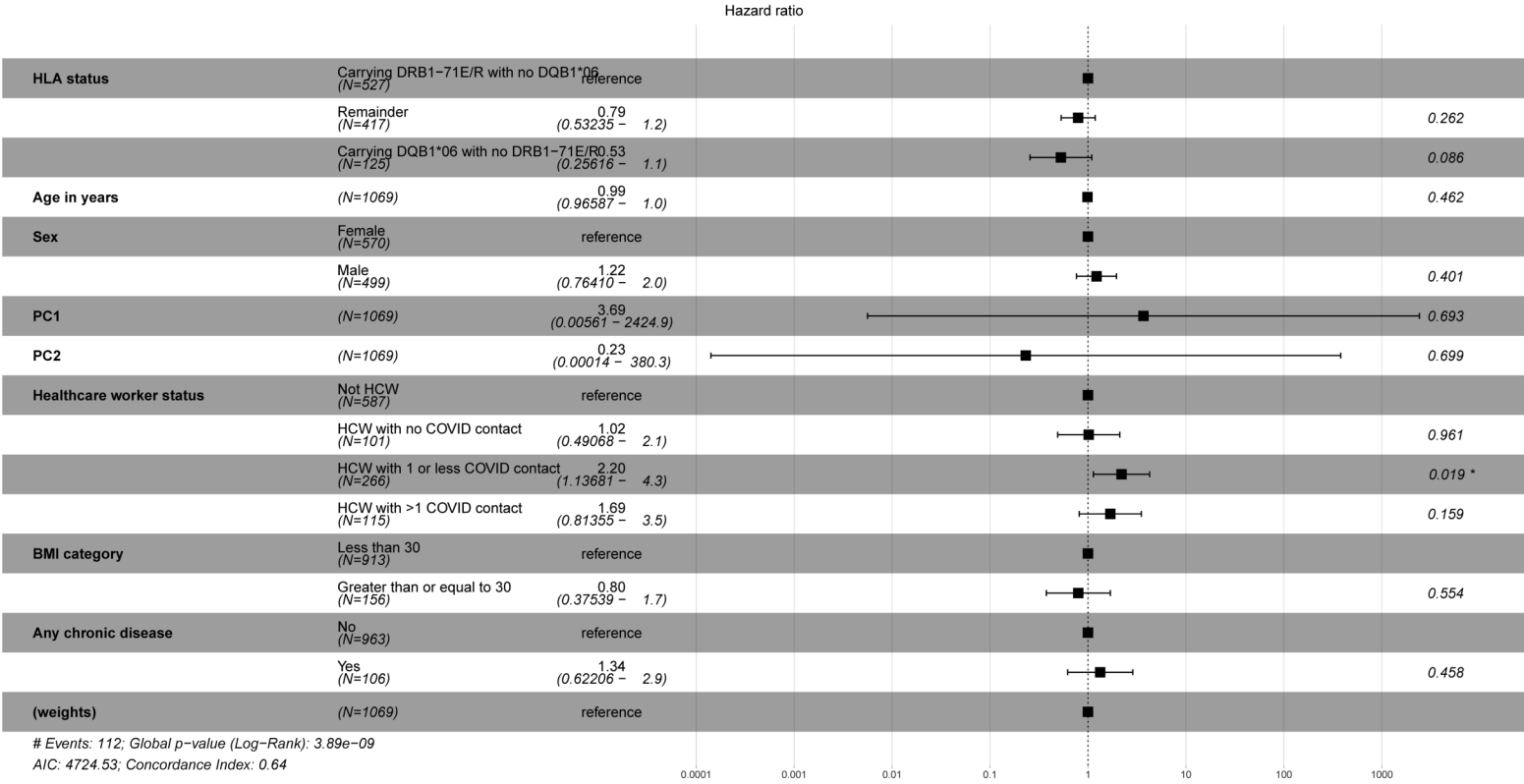


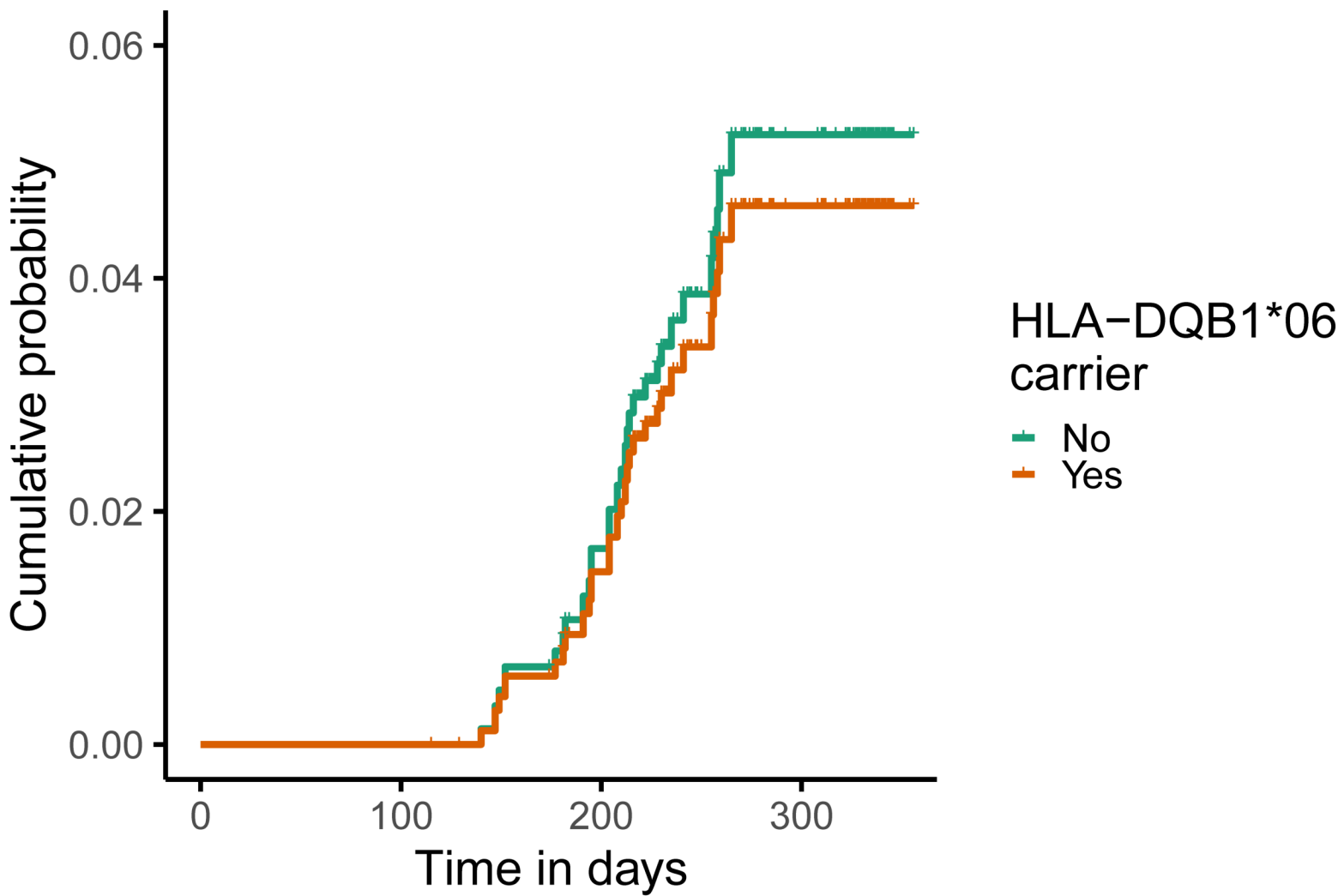
F





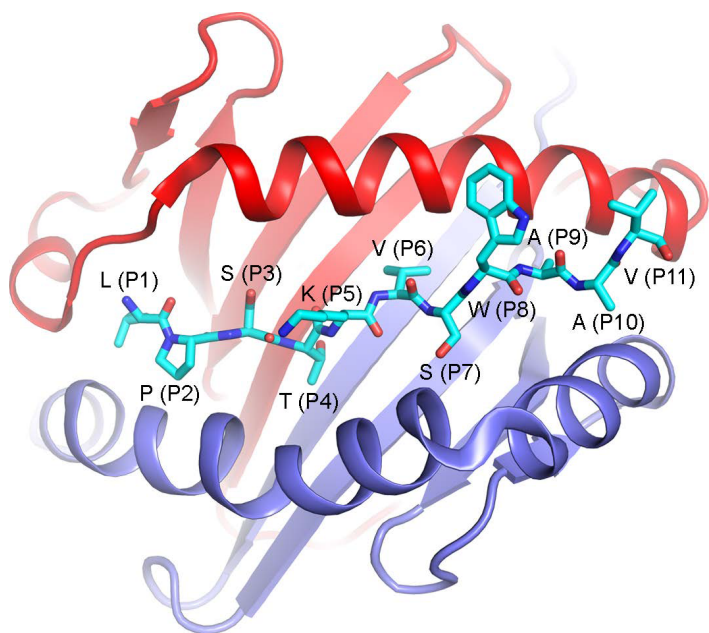




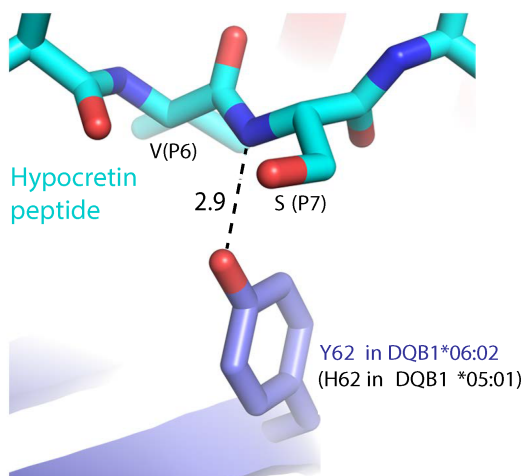


A

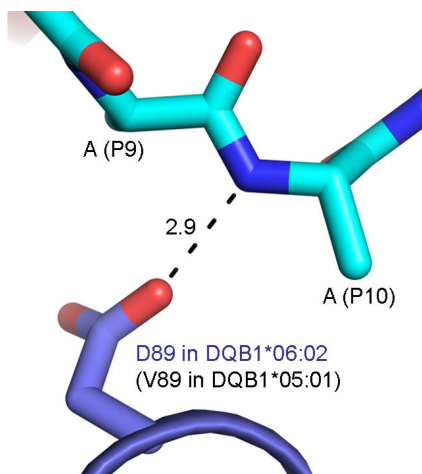
DQA1\*01:02-DQB1\*06:02-hypocretin peptide (crystal)



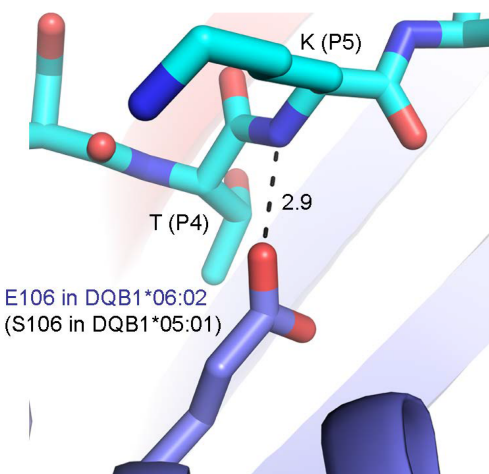
B



C



D



## Reporting Summary

Nature Portfolio wishes to improve the reproducibility of the work that we publish. This form provides structure for consistency and transparency in reporting. For further information on Nature Portfolio policies, see our [Editorial Policies](#) and the [Editorial Policy Checklist](#).

### Statistics

For all statistical analyses, confirm that the following items are present in the figure legend, table legend, main text, or Methods section.

n/a Confirmed

- ☐ ☒ The exact sample size ( $n$ ) for each experimental group/condition, given as a discrete number and unit of measurement
- ☐ ☒ A statement on whether measurements were taken from distinct samples or whether the same sample was measured repeatedly
- ☐ ☒ The statistical test(s) used AND whether they are one- or two-sided  
*Only common tests should be described solely by name; describe more complex techniques in the Methods section.*
- ☐ ☒ A description of all covariates tested
- ☐ ☒ A description of any assumptions or corrections, such as tests of normality and adjustment for multiple comparisons
- ☐ ☒ A full description of the statistical parameters including central tendency (e.g. means) or other basic estimates (e.g. regression coefficient) AND variation (e.g. standard deviation) or associated estimates of uncertainty (e.g. confidence intervals)
- ☐ ☒ For null hypothesis testing, the test statistic (e.g.  $F$ ,  $t$ ,  $r$ ) with confidence intervals, effect sizes, degrees of freedom and  $P$  value noted  
*Give  $P$  values as exact values whenever suitable.*
- ☐ ☒ For Bayesian analysis, information on the choice of priors and Markov chain Monte Carlo settings
- ☐ ☒ For hierarchical and complex designs, identification of the appropriate level for tests and full reporting of outcomes
- ☐ ☒ Estimates of effect sizes (e.g. Cohen's  $d$ , Pearson's  $r$ ), indicating how they were calculated

*Our web collection on [statistics for biologists](#) contains articles on many of the points above.*

### Software and code

Policy information about [availability of computer code](#)

#### Data collection

PLINK (version 1.9, <https://www.cog-genomics.org/plink/>)  
Multi-Ethnic HLA reference panel (version 1.0, 2021, <https://imputationserver.readthedocs.io/en/latest/reference-panels/>)

#### Data analysis

PLINK (version 1.9, <https://www.cog-genomics.org/plink/>)  
DosageConverter (version 1.0.4, <https://genome.sph.umich.edu/wiki/DosageConverter>)  
PHASE (version 2.1.1, <https://stephenslab.uchicago.edu/phase/download.html>)  
AlphaFold (<https://colab.research.google.com/github/sokrypton/ColabFold/blob/main/AlphaFold2.ipynb>)  
PyMOL Molecular Graphics System (version 2.3.2, <https://pymol.org/2/>)  
GCTA (version 1.24.4, <https://yanglab.westlake.edu.cn/software/gcta/#Overview>)  
R (version 4.1.1; packages: ipw, ggplot2, survminer, survival, perm, )  
R (version 3.6.2; GenABEL package)

For manuscripts utilizing custom algorithms or software that are central to the research but not yet described in published literature, software must be made available to editors and reviewers. We strongly encourage code deposition in a community repository (e.g. GitHub). See the Nature Portfolio [guidelines for submitting code & software](#) for further information.

## Data

Policy information about [availability of data](#)

All manuscripts must include a [data availability statement](#). This statement should provide the following information, where applicable:

- Accession codes, unique identifiers, or web links for publicly available datasets
- A description of any restrictions on data availability
- For clinical datasets or third party data, please ensure that the statement adheres to our [policy](#)

The datasets generated during and/or analysed during the current study are available from the corresponding author on reasonable request.

## Human research participants

Policy information about [studies involving human research participants and Sex and Gender in Research](#).

Reporting on sex and gender

The biological attribute of sex was used in this study. The justification for this is that biological sex was used as sample quality control metric, and the sex attribute used in analysis was derived from the genetic data.

Population characteristics

**\*\*Discovery cohort\*\***

The participants were enrolled in phase 1/2 (COV001) or phase 2/3 (COV002) randomized single-blind ChAdOx1 nCoV-19 (AZD1222) vaccine multi-centre efficacy trials conducted across multiple sites within the United Kingdom (NCT04324606, NCT04400838). In brief, following written informed consent adults aged 18 years and older were randomly assigned to receive either intramuscular ChAdOx1 nCoV-19 (AZD1222) or a control vaccine (MenACWY), to assess the safety and efficacy of the ChAdOx1 nCoV-19 vaccine against SARS-CoV-2.

**\*\*Replication cohort\*\***

The replication cohort was comprised of participants from three COVID-19 vaccine trials conducted across several sites within the United Kingdom. Two of these trials (COMCOV and COMCOV2) were in adults aged 50 years and older, randomised to receive homologous or heterologous two-dose schedules of either intramuscular ChAdOx1 nCoV-19, mRNA vaccines (BNT162b2 or mRNA-1273) or a nanoparticle vaccine (NVX-CoV2373). The other trial (COV006) was in children aged 6-17 who were randomised to receive either intramuscular ChAdOx1 nCoV-19 or a control vaccine (capsular group B meningococcal vaccine, 4CMenB).

Recruitment

The participants were recruited from COVID-19 vaccine trials conducted across several sites within the United Kingdom. They were randomised into vaccine groups.

Ethics oversight

The trials were conducted according to the principles of Good Clinical Practice and approved by the South Central Berkshire Research Ethics Committee (20/SC/0145, 20/SC/0179, 21/SC/0119, 21/SC/0022 and 21/SC/0054) and the UK regulatory agency (the Medicines and Healthcare products Regulatory Agency). We obtained informed consent from participants (or parent/guardians) for genetic data to be analysed, this was an optional consent in their clinical study consent forms.

Note that full information on the approval of the study protocol must also be provided in the manuscript.

## Field-specific reporting

Please select the one below that is the best fit for your research. If you are not sure, read the appropriate sections before making your selection.

☒ Life sciences ☐ Behavioural & social sciences ☐ Ecological, evolutionary & environmental sciences

For a reference copy of the document with all sections, see [nature.com/documents/nr-reporting-summary-flat.pdf](https://www.nature.com/documents/nr-reporting-summary-flat.pdf)

## Life sciences study design

All studies must disclose on these points even when the disclosure is negative.

Sample size

No formal sample-size calculation were conducted for this genetic analysis, rather sample size was based on the opportunistic sample availability from COVID-19 vaccine trials (genetic analysis was an exploratory endpoint in these studies).

Data exclusions

Genetic samples were removed if they had high genotyping missingness, genetic sex did not match reported sex or they had high heterozygosity — these are metrics of poor sample or genotyping quality. Individuals were excluded if they had estimates  $\geq 0.9$  identity by descent, excluding the individual with the highest SNP missingness rate from each pair preferentially — to remove duplicated samples.

Replication

An independent cohort was used to replicate findings.

Randomization

Participants were randomised into vaccine groups.



Blinding

Participants were blinded to their vaccine allocation.

## Reporting for specific materials, systems and methods

We require information from authors about some types of materials, experimental systems and methods used in many studies. Here, indicate whether each material, system or method listed is relevant to your study. If you are not sure if a list item applies to your research, read the appropriate section before selecting a response.

### Materials & experimental systems

n/a	Involved in the study
<input checked="" type="checkbox"/>	<input type="checkbox"/> Antibodies
<input checked="" type="checkbox"/>	<input type="checkbox"/> Eukaryotic cell lines
<input checked="" type="checkbox"/>	<input type="checkbox"/> Palaeontology and archaeology
<input checked="" type="checkbox"/>	<input type="checkbox"/> Animals and other organisms
<input type="checkbox"/>	<input checked="" type="checkbox"/> Clinical data
<input checked="" type="checkbox"/>	<input type="checkbox"/> Dual use research of concern

### Methods

n/a	Involved in the study
<input checked="" type="checkbox"/>	<input type="checkbox"/> ChIP-seq
<input checked="" type="checkbox"/>	<input type="checkbox"/> Flow cytometry
<input checked="" type="checkbox"/>	<input type="checkbox"/> MRI-based neuroimaging

## Clinical data

Policy information about [clinical studies](#)

All manuscripts should comply with the ICMJE [guidelines for publication of clinical research](#) and a completed [CONSORT checklist](#) must be included with all submissions.

Clinical trial registration	NCT04324606; NCT04400838; ISRCTN registry, 69254139 (EudraCT 2020-005085-33); ISRCTN Number: 27841311 (EudraCT Number: 2021-001275-16), ISRCTN Number: 15638344 (EudraCT number:2020-005765-13)
Study protocol	COV001 ( <a href="https://clinicaltrials.gov/ct2/show/NCT04324606">https://clinicaltrials.gov/ct2/show/NCT04324606</a> ); COV002 ( <a href="https://clinicaltrials.gov/ct2/show/NCT04400838">https://clinicaltrials.gov/ct2/show/NCT04400838</a> ); COMCOV ( <a href="https://comcovstudy.org.uk/files/com-covprotocolv9220-sept-2021cleanpdf">https://comcovstudy.org.uk/files/com-covprotocolv9220-sept-2021cleanpdf</a> ); COMCOV2 ( <a href="https://comcovstudy.org.uk/files/com-cov2protocolv6122-sep-2021cleanpdf">https://comcovstudy.org.uk/files/com-cov2protocolv6122-sep-2021cleanpdf</a> ); COV006 ( <a href="https://www.isrctn.com/ISRCTN15638344">https://www.isrctn.com/ISRCTN15638344</a> )
Data collection	The participants were recruited from COVID-19 vaccine trials conducted across several sites within the United Kingdom. Data between April 2020 and January 2022 were included in this manuscript.
Outcomes	Genetic analyses were included as exploratory outcome in the clinical trials from which these data were generated.